



**HAL**  
open science

## Insights into the roles of the Sideroflexins / SLC56 family in iron homeostasis and iron-sulfur biogenesis

Nesrine Tifoun, José de Las Heras, Arnaud Guillaume, Sylvina Bouleau,  
Bernard Mignotte, Nathalie Le Floch

► **To cite this version:**

Nesrine Tifoun, José de Las Heras, Arnaud Guillaume, Sylvina Bouleau, Bernard Mignotte, et al..  
Insights into the roles of the Sideroflexins / SLC56 family in iron homeostasis and iron-sulfur biogenesis.  
In press. hal-03085941v1

**HAL Id: hal-03085941**

**<https://uvsq.hal.science/hal-03085941v1>**

Preprint submitted on 22 Dec 2020 (v1), last revised 21 Jan 2021 (v2)

**HAL** is a multi-disciplinary open access archive for the deposit and dissemination of scientific research documents, whether they are published or not. The documents may come from teaching and research institutions in France or abroad, or from public or private research centers.

L'archive ouverte pluridisciplinaire **HAL**, est destinée au dépôt et à la diffusion de documents scientifiques de niveau recherche, publiés ou non, émanant des établissements d'enseignement et de recherche français ou étrangers, des laboratoires publics ou privés.



1 Review

# 2 Insights into the roles of the Sideroflexins / SLC56 3 family in iron homeostasis and iron-sulfur biogenesis

4 Nesrine Tifoun <sup>1†</sup>, José M. De las Heras <sup>1†</sup>, Arnaud Guillaume <sup>1</sup>, Sylvina Bouleau <sup>1</sup>, Bernard Mi-  
5 gnotte <sup>1,2</sup> and Nathalie Le Floch <sup>1,3\*</sup>

6 <sup>1</sup> Université Paris-Saclay, UVSQ, LGBC, 78000, Versailles, France.

7 <sup>2</sup> École Pratique des Hautes Études, PSL University, 75014, Paris, France

8 <sup>3</sup> IUT de Vélizy/campus de Rambouillet, GCGP Department, 19, allée des Vignes,  
9 78120 Rambouillet, France

10 \* Correspondence: [nathalie.leleu@uvsq.fr](mailto:nathalie.leleu@uvsq.fr)

11 <sup>#</sup> These authors equally contributed to this work.

12 **Abstract:** Sideroflexins (SLC56 family) are highly conserved multi-spanning  
13 transmembrane proteins inserted in the inner mitochondrial membrane in eu-  
14 karyotes. Few data are available on their molecular function but, since their first  
15 description, they were thought to be metabolite transporters probably required  
16 for iron utilization inside the mitochondrion. Such as numerous mitochondrial  
17 transporters, sideroflexins remain poorly characterized. The prototypic mem-  
18 ber SFXN1 has been recently identified as the previously unknown mitochon-  
19 drial transporter of serine. Nevertheless, pending questions on the molecular  
20 function of sideroflexins remain unsolved, especially their link with iron me-  
21 tabolism. Here, we review the current knowledge on sideroflexins, their pre-  
22 sumed mitochondrial functions and the sparse - but growing - evidence linking  
23 sideroflexins to iron homeostasis and iron-sulfur cluster biogenesis. Since an  
24 imbalance in iron homeostasis can be detrimental at the cellular and organismal  
25 levels, we also investigate the relationship between sideroflexins, iron and  
26 physiological disorders. Investigating Sideroflexins' functions constitutes an  
emerging research field of great interest and will certainly lead to main discov-  
eries on mitochondrial physiopathology.

27  
28 **Citation:** Lastname, F.; Lastname, F.  
29 Last-name, F. Title. *Biomedicines*  
30 2021, 9, x.  
31 <https://doi.org/10.3390/xxxxx>  
32 Accepted: date  
Published: date

**Keywords:** sideroflexin; mitochondria; mitochondrial transporters; iron home-  
ostasis; iron-sulfur cluster; heme biosynthesis; one-carbon metabolism; ferro-  
ptosis; ferritinophagy.

**Publisher's Note:** MDPI stays neu-  
tral with regard to jurisdictional  
claims in published maps and insti-  
tutional affiliations.



**Copyright:** © 2020 by the authors.  
Submitted for possible open access  
publication under the terms and  
conditions of the Creative Commons  
Attribution (CC BY) license  
(<http://creativecommons.org/licenses/by/4.0/>).

## 35 1. Sideroflexins: from structure to function

### 36 1.1. Sideroflexins from an historical point of view

37 The mitochondrion is at the crossroad of key metabolic pathways  
38 (energy metabolism, central carbon metabolism, one carbon metabo-  
39 lism, lipid, nucleotides and amino acids synthesis, etc.) and is a key  
40 player in cell fate and response to stress or infection. In order to ensure  
41 its essential functions within the cell, the mitochondrion requires a  
42 wide variety of enzymes and transporters. Among these proteins,  
43 sideroflexins (SFXN) form a family of recently discovered mitochon-  
44 drial proteins whose cell functions are progressively being specified.  
The first mention of the name "sideroflexin" appeared in 2001 [1]. Since  
then, a few studies have been dedicated to SFXN proteins and, at the

45 time we are writing this review, only 24 articles are retrieved in Pub-  
46 med using the keyword “sideroflexin”. Pioneers in the SFXN field,  
47 Fleming *et al.* identified a mutation affecting the *Sfxn1* gene in the *flexed-*  
48 *tail* mouse and emitted the hypothesis that the loss of *Sfxn1* was respon-  
49 sible for the sideroblastic anemia phenotype. However, it should be no-  
50 ticed that the causal link between the mutation in the *Sfxn1* gene and  
51 the phenotype of *flexed-tail* mice has not been clearly established yet. It  
52 was even questioned following a study showing that *flexed-tail* mice  
53 also had a mutation of the *Madh5/Smad5* gene, involved in the BMP  
54 pathway, which could explain the anemia and *flexed-tail* phenotype  
55 [2,3]. Anyway, SFXN own their name to the mice in which they were  
56 discovered (SIDEROblastic anemia and FLEXed-tail mouse) [1].

### 57 1.2. The Sideroflexin family: from genes to proteins

58 Sideroflexins (forming the SFXN/SLC56 family of mitochondrial  
59 transporters [4]) are highly conserved throughout eukaryotes. Only one  
60 sideroflexin is found in yeast (Fsf1 for Fungal sideroflexin 1), whereas  
61 there are two SFXNs in *Drosophila* (dSfxn1/3 and dSfxn2) and five SFXN  
62 (SFXN1-5) in vertebrates [1,5–7]. Our purpose is not to give an exten-  
63 sive overview of SFXN tissue distribution in this review, but some data  
64 are available in the literature. For example, SFXN1 mRNA levels in nor-  
65 mal tissues and human cancers, as well as tissue distribution of the five  
66 human SFXN, are available in [8].

67 SFXNs homologues display a high amino acid identity rate in  
68 mouse [1], xenopus [5] and human [8]. In humans, SFXN1 and SFXN3  
69 share 76.56% identical amino acids whereas there is 56.05% identity be-  
70 tween SFXN1 and SFXN2 and only 22.04% between SFXN1 and SFXN4.  
71 An alignment of human SFXNs is shown in **Figure 1**. Identity rates be-  
72 tween the different human, *Drosophila* and yeast sideroflexins proteins  
73 are described elsewhere [8,9]. The high degree of homology between  
74 SFXNs, especially between SFXN1 and SFXN3 in humans, suggest that  
75 sideroflexins may ensure redundant functions, as it was proposed for  
76 the mitochondrial import of serine that seems to be mediated by SFXN1  
77 [8]. This function will be evoked in more details below (see the section  
78 dedicated to the role of SFXN in regulating mitochondrial metabolism).  
79 Among the five mammalian SFXNs, SFXN4 is the most divergent mem-  
80 ber suggesting that this member do not share the same functions (**Fig-**  
81 **ure 1**). Indeed SFXN4 was not able to suppress defects caused by the  
82 concomitant loss of SFXN1 and SFXN3 in mammalian cells [8]. Inter-  
83 estingly, up to date no study has been done to specifically uncover Fsf1  
84 function. Because of the high degree of similarity between fungal  
85 sideroflexin and SFXN proteins from higher eukaryotes, we think that  
86 studies on the functions of Fsf1 will certainly lead to huge advances in  
87 the SFXN field and maybe reveal a general function for this family of  
88 proteins.

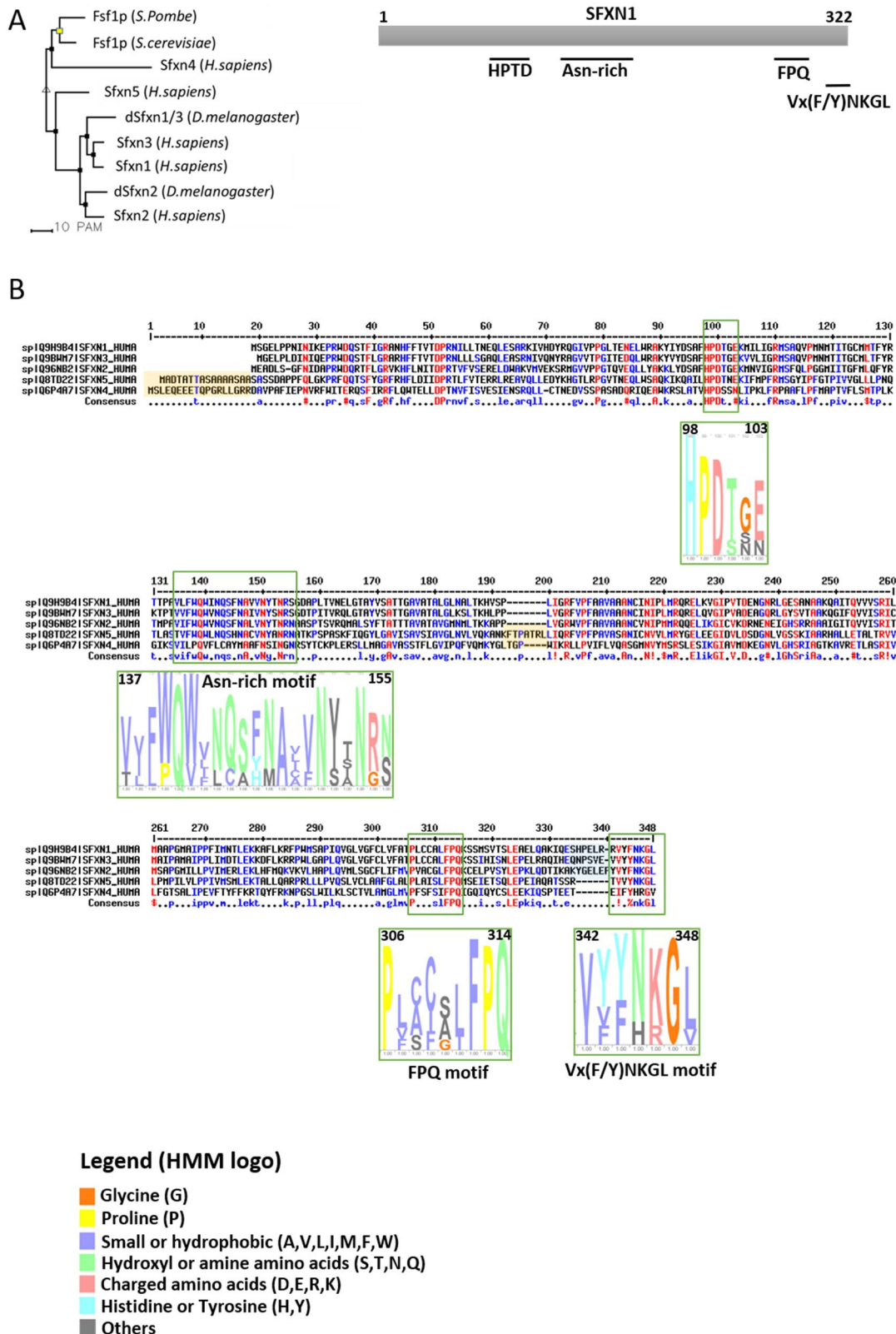


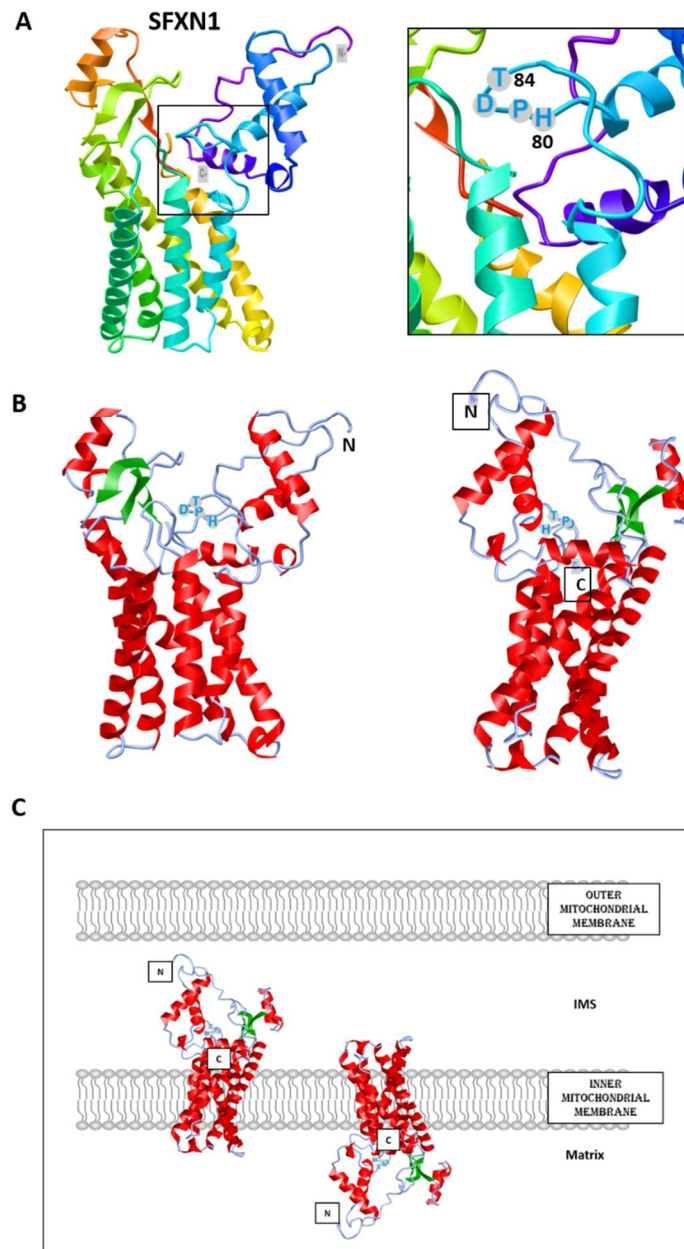
**Figure 1.** SFXNs form a family of conserved proteins in *Eukarya*. **A.** Left panel: Phylogenetic tree obtained using the MultiAlin software (<http://multalin.toulouse.inra.fr/multalin/>) [12]. Right panel: scheme of the SFXN1 protein and its conserved motifs. **B.** Alignment of human SFXNs protein sequences. Red amino acids are for high consensus levels (90%), the blue ones are for low consensus levels (50%). Meaning of symbols found in the consensus line: “!” is for Ile or Val, “\$” is for Leu or Met, “%” is for Phe or Tyr, “#” is anyone of Asn, Asp, Glu, Gln. Conserved motifs are shown and highlighted using an HMM logo created using Skyline (<http://skylign.org/>) with consensus colors for amino acids according to the ClustalX coloring scheme.

89  
90  
91  
92  
93  
94  
95  
96  
97

### 1.3. Sideroflexins are mitochondrial transporters implicated in one-carbon metabolism

SFXNs possess four to six predicted transmembrane domains composed by  $\alpha$ -helices revealed by *in silico* modeling [1,6,7]. These proteins share several highly conserved motifs including a HPDT motif and an asparagine-rich sequence (**Figure 1**) [1,6]. The functions of those conserved motifs have not been uncovered yet. Recently, Gyimesi and Hediger performed an *in silico* analysis of human SFXN1-5 sequences and described six well-conserved regions that could be important for SFXNs activity [10]. Whether these conserved regions are essential for metabolite transport need to be further confirmed at the bench.

To date, no crystal structure has been released for SFXNs. We thus tried to model SFXN tridimensional structure using the trRosetta software [11]. SFXN1 predicted structure is shown in **Figure 2**. Interestingly, this structure reveals six internal alpha helices that may correspond to the transmembrane domain of SFXN1.



115  
116  
117  
118  
119  
120  
121  
122  
123  
124  
  
125  
126  
127  
128  
129  
130  
131  
132  
133  
134  
135  
136  
137  
138  
139  
140  
141  
142  
143

**Figure 2. Predicted structure of human SFXN1. Structure prediction was obtained using trRosetta.** The confidence of the predicted model shown here is very high (with estimated TM-score=0.806). The model was built by trRosetta based on *de novo* folding, guided by deep learning restraints. iCn3D was used for the visualization of 3D structure [26]. A. SFXN1 predicted structure reveals several alpha helices and beta strands. N and C termini are labelled. The inset shows the position of the HPDT motif (aa 80-83), located just after the fourth helix. B. Two views highlighting secondary structures (helices in red, beta sheets in green). C. Models for SFXN1 insertion in the inner mitochondrial membrane.

SFXN1 topology was recently investigated by APEX and classical biochemical experiments [13–15]. Acoba *et al.* [15] performed detergent extraction and protease-protection assays on HEK human cells and confirmed that endogenous SFXN1 is a mitochondrial protein inserted in the inner mitochondrial membrane (IMM). Furthermore, evidence was given for the presence of N-terminus in the intermembrane space (IMS) but not in the matrix contrarily to what is predicted by a *in silico* analysis using Protter. According to biochemical data, the C-terminus seems to protrude in the matrix, in agreement with the previously proposed 5 transmembrane domains. However, our model is rather in agreement with a TM domain composed of six alpha helices and, if this predicted structure is correct, N and C termini could be in the same mitochondrial compartment (**Figure 2**). CryoEM structure of SFXN1 is thus needed to precise the three-dimensional structure of this carrier. Moreover, two recent studies investigated the mechanisms of SFXN1 mitochondrial import and shed light on the role of TIM22 and AGK2 in this process [16,15]. Evidence for a mitochondrial localization of SFXN are listed in the **Table 1**.

144

**Table 1.** Evidence for a mitochondrial localization of Sideroflexins.

| SFXN  | Model                                             | Localization | Experiment                                                                                                     | Reference                               |
|-------|---------------------------------------------------|--------------|----------------------------------------------------------------------------------------------------------------|-----------------------------------------|
| SFXN1 | Mouse                                             | IMM          | Co-fractionation                                                                                               | Fleming <i>et al.</i> , 2001 [1]        |
|       | Human cells<br>(Jurkat, K562)                     |              | Immunoblot on affinity-purified mitochondria<br>STED (co-localization of Flag-SFXN1 and COX4)                  | Kory <i>et al.</i> , 2018 [8]           |
|       | Human cells (MCF7, HT1080),<br><i>Drosophila</i>  |              | Immunoblot on mitochondrial extracts (fractionation)<br>Confocal microscopy, Proteomics (LC-MS/MS on SFXN1 IP) | Our unpublished data                    |
|       | Human cells (HEK)                                 |              | SILAC-based proteomics coupled LC-MS/MS, carbonate extraction, dig-<br>itonin fractionation                    | Acoba <i>et al.</i> , 2020 [15]         |
| SFXN2 | Human cells (HeLa)                                | OMM          | Confocal microscopy (Tom20 co-localization)                                                                    | Mon <i>et al.</i> , 2018 [9]            |
|       | Human cells<br>(Jurkat, K562)                     |              | Immunoblot on affinity-purified mitochondria                                                                   | Kory <i>et al.</i> , 2018 [8]           |
|       | Human cells (HEK)                                 |              | SILAC-based proteomics coupled LC-MS/MS                                                                        | Acoba <i>et al.</i> , 2020 [15]         |
| SFXN3 | Rat embryonic brain cells                         | IMM          | Fractionation, Confocal microscopy (co-localization with COX4), TEM                                            | Rivell <i>et al.</i> , 2019 [27]        |
|       | Human cells (Jurkat, K562)                        |              | Immunoblot on affinity-purified mitochondria                                                                   | Kory <i>et al.</i> , 2018 [8]           |
|       | Human cells (HEK)                                 |              | SILAC-based proteomics coupled LC-MS/MS                                                                        | Acoba <i>et al.</i> , 2020 [15]         |
|       | Human cells (HeLa)                                | IMM          | Fractionation and protease protection assay                                                                    | Hildick-Smith <i>et al.</i> , 2013 [28] |
| SFXN4 | Human cells (Jurkat, K562)                        |              | Immunoblot on affinity-purified mitochondria                                                                   | Kory <i>et al.</i> , 2018 [8]           |
|       | Human cells (HEK)                                 |              | SILAC-based proteomics coupled LC-MS/MS                                                                        | Acoba <i>et al.</i> , 2020 [15]         |
|       | Human cells (HEK)                                 |              | SILAC-based proteomics coupled LC-MS/MS                                                                        | Acoba <i>et al.</i> , 2020 [15]         |
| SFXN5 | Human cells (HEK)                                 |              | SILAC-based proteomics coupled LC-MS/MS                                                                        | Acoba <i>et al.</i> , 2020 [15]         |
|       | Mouse astrocytes, human cortex<br>and spinal cord |              | Immunocapture of GFP-OMM-tagged mitochondria (MitoTag mice),<br>immunostaining                                 | Fecher <i>et al.</i> , 2019 [29]        |

145

<sup>1</sup>IMM: inner mitochondrial membrane, IP: immunoprecipitation, OMM: outer mitochondrial membrane, STED: stimulated emission depletion, TEM: Transmission Electron Microscopy, SILAC: Stable isotope labelling of amino acids, LC-MS/MS: Liquid chromatography and tandem mass spectrometry.

146

147

148 Because of their predicted structure, showing several hydrophobic  
149 alpha helices, and their mitochondrial location, sideroflexins were pro-  
150 posed to be mitochondrial metabolite transporters. Rat Sfxn3 was pre-  
151 sumed to be a tricarboxylate carrier (TCC) and, later, Sfxn5 (also known  
152 as BBG-TCC ) was reported to transport citrate *in vitro* [17,18]. How-  
153 ever, it is only recently that a function of mitochondrial serine trans-  
154 porter was reported for SFXN1 [8].

155 By a bioinformatic analysis, the *S. cerevisiae* Fsf1 (YOR271cp) was  
156 proposed to be a candidate alpha-isopropylmalate transporter but no  
157 experimental data ascertained this function [19]. Similarly, the pre-  
158 dicted Fsf1 protein from *Schizosaccharomyces pombe*, Spac17g6.15c, is  
159 annotated as a serine transporter in the database Pombase  
160 (<https://www.pombase.org/>) based on its homology with human  
161 SFXN1 [20,21], although it has not been extensively studied.

162 Since mice lacking Sfxn1 present similar features to that observed  
163 in human syndromes caused by a lack of pyridoxine or ALAS2 muta-  
164 tion (X-linked sideroblastic anemia), it was also proposed that Sfxn1  
165 transports pyridoxine (B6 vitamin) inside the mitochondria [1,22]. Since  
166 pyridoxine is the precursor of pyridoxal phosphate that serves as a co-  
167 factor for ALAS2 (the erythroid specific enzyme catalyzing the first step  
168 of heme biosynthesis), SFXN1 could thus directly regulate heme bio-  
169 synthesis. However, it has been recently reported that human SFXN1 is  
170 not able to transport pyridoxine *in vitro* [8]. Even if we cannot exclude  
171 that SFXN1 functions in a complex that is not fully reconstituted in  
172 *in vitro* assays, SFXN1 may not be the carrier for pyridoxine. Mtm1p,  
173 SLC25A39 yeast homologue, was suggested to import pyridoxal 5'-  
174 phosphate inside the mitochondria [23,24]. However, the substrate  
175 specificity of the SLC25A39 carrier remains unknown [25].

176 Thus, the main role of Sfxn1 seems to be the mitochondrial serine  
177 import. Inside the mitochondrion, Serine can be catabolized by the ser-  
178 ine hydroxymethyl transferase (SHMT2) into glycine, an amino acid  
179 necessary for ALA synthesis (see below). So, the lack of Sfxn1 would  
180 lead to decreased mitochondrial levels of serine and glycine leading to  
181 ALA synthesis impairment (see section 4).

#### 182 1.4. Sideroflexins in disease

183 Hildick-Smith *et al.* described for the first time a human syndrome  
184 (combined oxidative phosphorylation deficiency-18, OMIM entry #  
185 615578), that was directly associated with the lack of a member of the  
186 Sfxn family, namely SFXN4 [28]. Patients showed macrocytic anemia  
187 and mitochondriopathy non-explainable by other causes but the lack of  
188 SFXN4. Recently, a third patient with SFXN4 mutations was described  
189 by Sofou *et al* [30]. The three patients with SFXN4 mutations presented  
190 with intrauterine growth retardation, mild to severe intellectual disa-  
191 bilities, microcephaly, , neonatal lactic acidosis, macrocytic anemia and  
192 severe visual impairment. Sofou *et al* reported optic nerve hypoplasia  
193 in the third case. More recently, some of the mechanisms that could ex-  
194 plain those effects in humans were reported in the K562 erythroleuke-  
195 mic cell line [31]. Interestingly SFXN4 loss-of-function leads to a general  
196 decrease in the levels of the respiratory chain complexes I-IV, which  
197 could be explained by an impaired Fe-S cluster synthesis, as evidenced  
198 by a Fe-S fluorescence assay (FeSFA). Nevertheless, Sofou *et al.* showed  
199 that the effect of SFXN4 decrease would be exclusively in Complex I  
200 but not in the rest of the respiratory chain complexes after muscle bi-



201  
202  
203  
204  
205  
206  
207  
208  
209  
210  
211  
  
212  
213  
214  
215  
216  
217  
218  
219  
220  
221  
222  
223  
224  
225  
226  
227  
228  
229

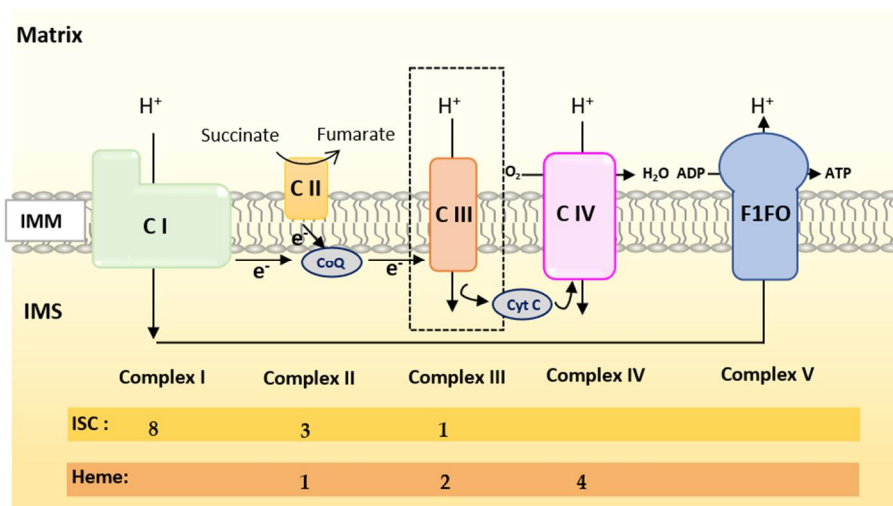
opsy [30]. Despite these discrepancies, which could be due to the different nature of the mutations analyzed in each case, it seems clear that Complex I activity is affected in both studies, which reinforces the hypothesis that *SFXN4* could have a role, either direct or indirect, on Fe-S biosynthesis.

Besides the description of mutations in the *SFXN4* human gene causing the COXPD18 syndrome, *SFXN4* was also reported to be a predisposition gene for familial colorectal cancer (CRC). Hence, rare *SFXN4* truncating variants were identified in 3/96 CRC familial cases [32]. An aberrant expression of *SFXN1* and *SFXN5* was also reported in patients with breast cancer or gliomas [33,34].

## 2. Sideroflexins and mitochondrial respiration

### 2.1. Overview of the mitochondrial respiratory complexes and the place of iron in RC

Oxidative Phosphorylation (OXPHOS) couples the transport of electrons (through a series of mitochondrial respiratory complexes containing redox-active prosthetic groups) to the production of ATP by the mitochondrial ATP synthase, commonly referred to as the complex V of respiratory chain (**Figure 3**). Respiratory complexes (RC) are arranged in supercomplexes (SC) and megacomplexes in the inner mitochondrial membrane [35,36]. The Electron Transport Chain (ETC) comprises four RC (Complex I-IV) containing more than 70 nuclear DNA encoded subunits and 13 mitochondrial DNA (mtDNA) encoded subunits, some of which including iron-sulfur clusters (ISCs) or heme; those iron-containing groups are essential cofactors for electron transport from one complex to another [37,38]. The purpose of this review is not to give an extensive overview of the abundant literature on RC, so we invite the reader to refer to recent reviews for details on the composition, structure and biogenesis of RC [35,38,39].



230  
231  
  
232  
233  
234  
235  
236

**Figure 3.** Scheme of the mitochondrial respiratory chain. ISC and heme indicate the respective number of ISC-containing subunits and heme in each complex.

Mammalian Complex I (NADH: Ubiquinone Oxidoreductase) is a L-shaped megastructure of about 1 MDa comprising 14 core subunits and up to 45 subunits. Among them, five essential subunits (NDUFV1, NUDFV2, NDUFS1, NDUFS7 and NDUFS8) bare the eight ISCs of CI (two [2Fe-2S] and six [4Fe-4S] clusters).

237 Mammalian Complex II, the smallest of the RC, is composed of  
238 only four subunits: succinate dehydrogenase [ubiquinone] flavoprotein  
239 (also known as Flavoprotein subunit of complex II, Fp, SDHA), succinate  
240 dehydrogenase [ubiquinone] iron-sulfur subunit (a Fe-S protein  
241 also named Ip or SDHB), the membrane-anchoring succinate dehydro-  
242 genase cytochrome b560 subunit (CybL, SDHC), and finally the succinate  
243 dehydrogenase [ubiquinone] cytochrome b small subunit (CybS,  
244 SDHD). These subunits are respectively encoded by the *SDHA*, *SDHB*,  
245 *SDHC* and *SDHD* nuclear genes. Fp/SDHA and Ip/SDHB are anchored  
246 to the IMM thanks to CybL/SDHC and CybS/SDHD that are the mem-  
247 brane-anchoring subunits of CII. Complex II contains three ICSs ([2Fe-  
248 2S], [4Fe-4S] and [3Fe-4S] in SDHB) and a heme shared by SDHC and  
249 SDHD.

250 Mammalian Complex III (also known as bc1 complex) is a dimer  
251 made of monomers containing 11 subunits among which three are es-  
252 sential redox subunits: cytochrome b, cytochrome c1 and the Fe-S pro-  
253 tein Cytochrome b-c1 complex subunit Rieske (Rieske, ISP, RISP, Rip1  
254 are alternative names that can be found in the literature for this pro-  
255 tein). Altogether, these catalytic subunits possess two heme b (Cyt b), a  
256 c-type heme (Cyt c1) and a [2Fe-2S] cluster (Rieske) [40]. Heme b is syn-  
257 thesized by Ferrochelatase (FECH) but the mechanism of its insertion  
258 into cytochrome b has not been fully elucidated [40].

259 Mammalian Complex IV contains three mitochondrially-encoded  
260 subunits (Cytochrome c oxidase subunit 1, 2 and 3) plus eleven sub-  
261 units encoded by the nuclear genome. CIV possesses four redox-active  
262 metal centers including heme a and heme a3 but no ISCs.

263 To summarize, Complex I is made of numerous subunits includ-  
264 ing 8 ISC-containing subunits but none containing heme. Complex IV  
265 presents 4 redox-active centers containing heme but no ISC. Both Com-  
266 plexes II and III have ISC and heme containing subunits.

## 267 2.2. Current knowledge on the regulation of mitochondrial respiration by 268 SFXN proteins

269 Kory *et al.* reported decreased basal respiration in SFXN1/SFXN3  
270 double knockout Jurkat cells [8]. Whereas SFXN1 loss alone is not det-  
271 rimental for respiration of intact cells [8,15], Acoba *et al.* reported a sig-  
272 nificant decrease in Oxygen Consumption Rates (OCR) of isolated mi-  
273 tochondria from HEK *SFXN1* KO cells with CI, CII and CIII substrates  
274 (pyruvate, Glu, Gln, dimethyl-  $\alpha$ -ketoglutarate, succinate and glycerol-  
275 3-phosphate) [15]. In human embryonic cells, the loss of SFXN1 leads  
276 to a marked decrease in the protein levels of three subunits of the Com-  
277 plex III and to a lesser extent in Complex II subunit SDHB (**Table 2**)  
278 [15]. SFXN4 KO leukemic cells also showed reduced levels of several  
279 RC subunits containing ISCs [31].

280 Whereas no significant change in the activity of the CI, CII and CIV  
281 ETC complexes was observed upon SFXN1 gene knockout in HEK cells,  
282 CIII activity was dramatically decreased and partially restored upon  
283 SFXN1 overexpression [15]. In agreement with the observed decrease  
284 in the levels of cytochrome b (MT-CYB), cytochrome b-c1 complex sub-  
285 unit 2 (UQCRC2) and cytochrome b-c1 complex subunit Rieske  
286 (UQCRFS1) subunits, Acoba *et al.* also reported a reduction in CIII2 and  
287 in CIII2-CIV subcomplex whereas the assembly of respiratory super-  
288 complexes was unaffected. Mitochondrial translation is not dramati-

289 cally impaired in the absence of a functional SFXN1 protein, neverthe-  
290 less a slight decrease in cytochrome b translation was reported in this  
291 study.

292 No decrease neither in the quantity of mtDNA nor in the mito-  
293 chondrial mass was seen in SFXN1 KO cells, thus a general defect in  
294 mitochondrial biogenesis can be excluded [8,15]. Current knowledge  
295 on Complex III biogenesis is well-described in [40]. Seven assembly fac-  
296 tors are implicated in CIII biogenesis in humans (UQCC1-3, CCHL,  
297 BCSL1, LYRM7 and TTC19). The Rieske subunit is first translocated  
298 from the cytosol to the matrix where it acquires its ISC and is further  
299 incorporated in CIII. In the matrix, Rieske is stabilized by the chaperone  
300 LYRM7 [41]. BCS1L is required for the translocation of the folded  
301 Rieske iron-sulfur protein in the IMM by a mechanism that remains  
302 largely unknown [42]. No regulation of the levels of BCSL1 and LYRM7  
303 assembly factors was observed when SFXN1 is absent in mammalian  
304 cells [15].

305 Interestingly, HEK *SFXN1*<sup>KO</sup> cells were reported to have markedly  
306 reduced levels of Coenzyme Q (CoQ, ubiquinone), a lipid of the IMM  
307 which accepts electron from CI and CII and then donates one electron  
308 to the ISC of the Rieske subunit and another one to the heme of the  
309 cytochrome b of CIII (see [40] and [43] for more details on the transfer  
310 of electrons from CoQ to the IMS soluble electron carrier cytochrome  
311 c).

312 Deficiencies of mitochondrial respiration and/or RC activity were  
313 also reported for other SFXN, as summarized in **Table 2**. For example,  
314 *SFXN2* knockout led to a decreased activity of CII-CIII and CIV [9]. As  
315 no specific impairment in complex III activity has been described nor  
316 in *SFXN2* nor in *SFXN4* KO cells, there is presumably no interaction  
317 between those SFXN isoforms and the BCS1L protein (responsible of  
318 the GRACILE Syndrome), a mitochondrial chaperone which is an-  
319 chored to the inner mitochondrial membrane and required for proper  
320 Complex III activity [44]. Nevertheless, this possibility cannot be totally  
321 discarded, as the patients with S78G point mutation in the BCS1L gene  
322 have no decreased Complex III activity when compared with other mu-  
323 tations of the same gene.

289  
290  
291  
292  
293  
294  
295  
296  
297  
298  
299  
300  
301  
302  
303  
304  
305  
306  
307  
308  
309  
310  
311  
312  
313  
314  
315  
316  
317  
318  
319  
320  
321  
322  
323  
324

325

**Table 2.** Consequences of SFXN deficiency on the ETC complexes.

| SFXN  | Model                                                                         | Complex                  | Data                                                                                                                                     | Reference                              |
|-------|-------------------------------------------------------------------------------|--------------------------|------------------------------------------------------------------------------------------------------------------------------------------|----------------------------------------|
| SFXN1 | HEK <i>SFXN1</i> <sup>KO</sup> cells<br>HeLa <i>SFXN1</i> <sup>KO</sup> cells | CI                       | No significant loss of activity<br>SDHB ↓                                                                                                | Acoba <i>et al</i> , 2020 [15]         |
|       |                                                                               | CII                      | No significant loss of activity<br>UQCRC2 ↓↓<br>UQCRFS1 ↓↓                                                                               |                                        |
|       |                                                                               | CIII                     | Cytochrome b ↓↓↓<br>Significant loss of activity<br>Reduced levels of CIII <sub>2</sub> and CIII <sub>2</sub> -CIV respiratory complexes |                                        |
| SFXN2 | HEK <i>SFXN2</i> <sup>KO</sup> cells                                          | CI<br>CII- CIII<br>CIV   | No significant loss of activity<br>Significant loss of activity<br>Significant loss of activity                                          | Mon <i>et al</i> , 2019 [9]            |
| SFXN3 | <i>SFXN3</i> KO mouse                                                         | CI, CIV                  | No significant loss of activity                                                                                                          | Amorim <i>et al</i> , 2017 [45]        |
| SFXN4 | Primary fibroblasts from two individuals with <i>SFXN4</i> mutations          | CI+CIII                  | Decreased activity                                                                                                                       | Hildick-Smith <i>et al</i> , 2013 [28] |
|       | <i>SFXN4</i> KD zebrafish                                                     | CI<br>CI+CIII            | Decreased activity                                                                                                                       | Sofou <i>et al</i> , 2019 [30]         |
|       | K562 <i>SFXN4</i> <sup>KO</sup> cells                                         | CI<br>CII<br>CIII<br>CIV | NDUFB8 ↓<br>SDHB ↓<br>UQCRC2 ↓<br>COX2 ↓                                                                                                 | Paul <i>et al</i> , 2019 [31]          |
| SFXN5 |                                                                               |                          | N.A. <sup>1</sup>                                                                                                                        |                                        |

<sup>1</sup> NA: Not addressed.

326

327

### 3. Which place for Sideroflexins in the regulation of mitochondrial metabolism?

#### 3.1. Sideroflexins and one-carbon metabolism (OCM)

Using CRISPR/Cas9 based-screening, Kory *et al.* uncovered a function of mitochondrial serine transporter for SFXN1 [8]. The import of serine inside mitochondria is a key step of the OCM, a major metabolic pathway coupled to the synthesis of methyl donors necessary for purine synthesis, epigenetic methylation processes and synthesis of neurotransmitters [46]. Moreover, glycine - arising from serine catabolism by the SHMT2 enzyme [47] - is a key amino acid for the synthesis of heme, a cofactor present in cytochromes of the respiratory chain and other essential proteins, such as CYP450 proteins. Finally, OCM is known as a central pathway ensuring hyperproliferation of cancer cells. Hence OCM, through the folate cycle, links serine catabolism to purine and nucleotides biosynthesis. Liver, kidney and blood are tissues with high OCM activity, however OCM role is not restricted to these organs but present in all human tissues including brain [46]. Actually, defective one-carbon metabolism during embryonic development is responsible for neural tube defects.

Whereas Jurkat cells lacking SFXN1 proliferate as wild-type cells do, their proliferation rate is markedly reduced in a medium lacking serine but is normal in the absence of glycine that can be provided by the catabolism of serine [8]. A lower proliferative rate compared to that of wild-type cells was also reported for HEK *SFXN1* KO cells in the absence of serine. Interestingly, proliferation of SFXN1 deficient cells was enhanced when formate (OCM metabolite), but not hemin (heme derivative), was added [15]. Additionally, Kory *et al.* showed that the double knockout of SFXN1 and SFXN3 greatly impaired proliferation in a glycine-deficient medium. Apart from human *SFXN4*, overexpression of virtually any *SFXN* family member including *S. cerevisiae* FSF1/YOR271C and the two *Drosophila* orthologues *dSfxn1* and *dSfxn2* can rescue the glycine auxotrophy due to the OCM defect induced by the concomitant loss of SFXN1 and SFXN3 in human leukemic cells. However, the defect in purine synthesis is rescued only by SFXN2, SFXN3, *dSfxn1* and *S. cerevisiae* FSF1 [8]. Thus, most SFXN appear functionally redundant in serine import although probably with different kinetic properties. Moreover, they might also ensure the mitochondrial import of other metabolites.

#### 3.2. Sideroflexins in central carbon metabolism

Disturbance of central carbon metabolism was reported in SFXN1-null cells. A LC-MS analysis of tricarbohylic acid (TCA) cycle metabolites contained in HEK *SFXN1* KO cells showed significantly reduced levels of citrate and isocitrate while  $\alpha$ -ketoglutarate ( $\alpha$ -KG) was decreased and succinate cellular levels were unchanged [15]. Isotopic labelling experiments helped understanding the role of SFXN1 in mitochondrial metabolism.  $^{13}\text{C}$  metabolic flux analysis ( $^{13}\text{C}$  MFA) is a useful tool to assess intracellular fluxes and get clues on the metabolic pathways that are differentially activated in mammalian cells depending of the genetic context or environmental conditions [48]. Using  $^{13}\text{C}$  MFA to investigate metabolic fluxes in HEK *SFXN1* KO cells, Acoba *et al* provided evidence for a reduced activity of the glutamate dehydrogenase (GDH) that converts Glu in  $\alpha$ -KG using NAD(P)<sup>+</sup> as a coenzyme [49,50]. The lower activity of GDH is unlikely due to a lowering in

381 NAD(P)<sup>+</sup> since NAD(P)<sup>+</sup>/NADPH ratio was unchanged in SFXN1-de-  
382 ficient cells [15]. In animals, GDH is regulated by a wide variety of lig-  
383 ands (NADH, GTP, ATP, palmitoyl-coA, steroid hormones, leucine)  
384 and the mitochondrial enzymes SIRT4 and SCHAD. Alanine ami-  
385 notransferase (ALT) activity is also markedly reduced in SFXN1-null  
386 cells [15]. This deficiency in alanine catabolism is probably due to the  
387 lower availability of  $\alpha$ -KG in SFXN1-null cells. Alanine aminotransfer-  
388 ase (also known as GPT) is implicated in L-alanine degradation via  
389 transaminase pathway and uses pyridoxal 5'-phosphate as a cofactor.  
390 A comprehensive review of nitrogen utilization and amino acid metab-  
391 olism can be found in [51]. Mitochondrial levels of GDH and ALT2 (mi-  
392 tochondrial alanine aminotransferase) were not investigated in SFXN1-  
393 deficient cells and we wonder if the absence of SFXN1 could trigger a  
394 decrease in the mitochondrial import or stability of some mitochondrial  
395 enzymes intervening in the catabolism of amino acids that fuel the TCA  
396 cycle. Acoba *et al* also performed <sup>13</sup>C MFA with [U-<sup>13</sup>C]-glucose to fuel  
397 the TCA cycle with [U-<sup>13</sup>C]-labelled acetyl-coA and provided evidence  
398 for an increase in the incorporation of glucose in the TCA cycle [15].

399 NAD<sup>+</sup>/NADH ratio was also increased in SFXN1 KO cells and, al-  
400 together, the results obtained by Acoba *et al* shed light on a disturbance  
401 of central carbon metabolism upon the loss of SFXN1. Whether the de-  
402 ficiency in SFXN1 orthologues and the other human sideroflexins also  
403 affects central carbon metabolism is an open question that is not fully  
404 elucidated.

#### 405 **4. Sideroflexins, iron homeostasis and heme biosynthesis**

##### 406 *4.1. A brief overview of iron homeostasis, ISCs and heme biosynthesis*

407 Iron is an essential cofactor for several enzymes involved in redox  
408 reactions due to its ability to exist in two ionic forms: ferrous iron (Fe<sup>2+</sup>)  
409 and ferric iron (Fe<sup>3+</sup>). Iron is thus easily oxidized and reduced which  
410 makes it suitable for redox reactions. Thus, iron is a key player in many  
411 important cellular processes, including energy metabolism, respiration  
412 and DNA synthesis. The implication of iron in all these processes is  
413 done through the incorporation of this atom in complex structures syn-  
414 thesized mainly in the mitochondria: iron-sulfur clusters and heme.  
415 Iron homeostasis is a tightly controlled process in which numerous pro-  
416 teins intervene [52–55]. **Figure 4** depicts the main actors of iron traffick-  
417 ing and metabolism at the cellular level.

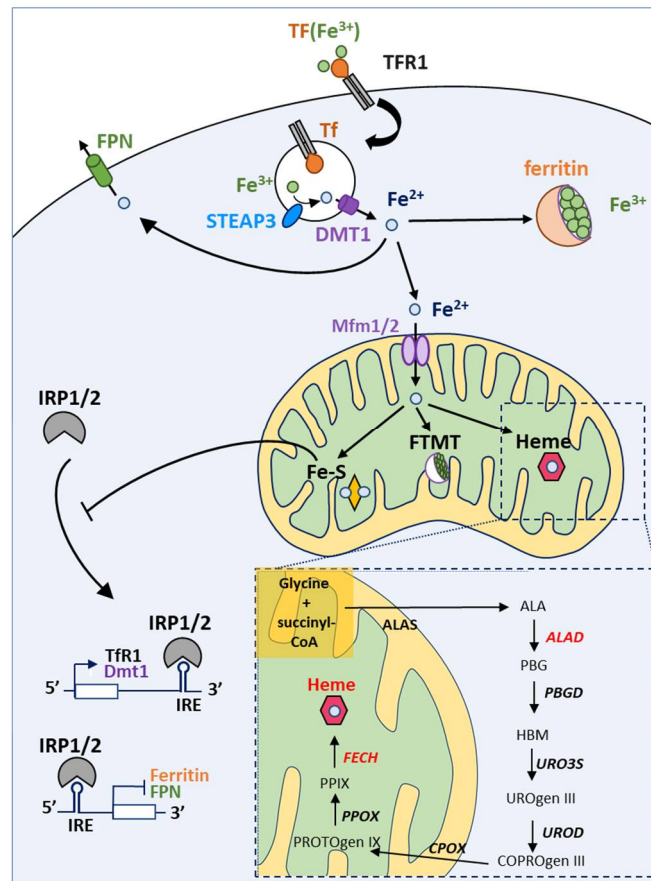


**Figure 4. Iron homeostasis and utilization at the cell level.** Iron cellular uptake is controlled by transferrin and its receptor (Tf and TFR1, respectively). Afterwards, in the endosome, iron is reduced thanks to the action of STEAP3 (which converts the insoluble  $\text{Fe}^{3+}$  to soluble  $\text{Fe}^{2+}$ ) and released from the endosome into the cytoplasm by the DMT1 channel. Free iron can be stored by ferritin in the cytoplasm or can be transported into the mitochondria, thanks to Mitoferrin 1 and 2 transporters (Mfrn1/2). Excess of iron is released out of the cell by Ferroportin (FPN). Inside the mitochondrion, iron can be stored in FTMT (mitochondrial ferritin) or incorporated in heme or Fe-S clusters. IRP1 and 2 (Iron Related Protein 1 and 2) are the major regulators of iron metabolism. In iron-depleted cells, IRP1 can bind IRE (Iron Response Elements) motifs to promote or repress mRNA translation. If IREs are located in the 5'UTR, IRP1 binding represses mRNA translation under low iron levels. On the contrary, transcripts with IREs at the 3'UTR are stabilized and translated upon IRP binding. Hence, low iron levels lead to decreased Ferritin and FPN levels but promote TFR1 and DMT1 synthesis. High levels of iron prevent IRP1 binding to IREs (see main text for details).

Maintaining iron homeostasis is essential for cell viability and iron intracellular levels are thus tightly controlled by Iron Regulatory Proteins (IRP1 / 2). IRP1/2 regulate the levels of key proteins intervening in iron homeostasis by binding to Iron Responsive Element (IRE) sequences either located in the 5'UTR or in the 3'UTR of mRNA encoding actors of iron metabolism. For example, when cellular iron levels are low, IRP proteins bind to IRE in the 5' UTR of ferritin and ferroportin mRNAs (among others) and thereby inhibit their translation. The IRPs proteins can also bind to IRE in the 3'UTR of iron-regulated mRNAs, such as TfR1 and DMT1 mRNAs encoding two proteins involved in iron uptake, thereby preventing endonuclease-mediated degradation of these mRNAs (see [56] for a review). Thus, this regulation by IRP

418

419

420

421

422

423

424

425

426

427

428

429

430

431

432

433

434

435

436

437

438

439

440

441

442

443

444

445

446

447

448 proteins under low iron concentration leads to an increase in iron up-  
449 take as well as a decrease in iron storage and export. On the opposite,  
450 under high iron levels, the synthesis of iron-sulfur clusters is enhanced.  
451 The binding of an iron-sulfur cluster to the IRP1 protein leads a confor-  
452 mational change inhibiting its IRE binding activity but promoting its  
453 aconitase activity. The ACO1 enzyme (*e.g.*, Fe-S bound IRP1) catalyzes  
454 the conversion of citrate and isocitrate in the cytosol enhancing, proba-  
455 bly, NADPH generation and lipid synthesis [57]. Our aim is not to give  
456 an extensive review of the IRE-IRP signaling pathway and numerous  
457 comprehensive reviews can be found elsewhere, such as in [58].

458 Iron-sulfur clusters are made up of iron and sulfur ions which  
459 come together to form [1Fe-0S], [2Fe-2S], [3Fe-4S] and [4Fe-4S] clusters  
460 [59]. Fe-S clusters (ISCs) are found in numerous metalloproteins such  
461 as aconitase 1 [54,60–62]. Thus, ISCs are involved in a wide variety of  
462 cellular processes among which we can cite the Krebs cycle, mitochon-  
463 drial respiration, DNA replication / repair. Assembly of the Fe-S center  
464 is carried out by the ISC machinery. Inorganic sulfur is first produced  
465 from the cysteine by the cysteine desulfurase NFS1. Then, the Fe-S clus-  
466 ter is formed on the ISC assembly enzyme (ISCU) with the help of  
467 frataxin (FXN) [63].

468 Heme is a complex of ferrous iron and protoporphyrin IX (PPIX).  
469 It is an important prosthetic group for many vital proteins, such as he-  
470 moglobin, myoglobin, cytochromes and CYP450 proteins [64,65]. Heme  
471 is involved in the transport and storage of oxygen, the transfer of elec-  
472 trons for enzymatic redox reactions, signal transduction, ligand bind-  
473 ing and control of gene expression [66]. Heme biosynthesis (**Figures 4,**  
474 **6**) is a pathway comprising eight steps, among which four arise inside  
475 the mitochondrion (*e.g.* the first and the last three steps). The rate lim-  
476 iting enzyme of this process is the ALA-synthase (ALAS) responsible  
477 for the synthesis of  $\delta$ -aminolevulinic acid (ALA) from the condensation  
478 of glycine and succinyl-CoA, in the presence of pyridoxal-5'-phosphate  
479 [67,68]. Two genes encode ALA-synthases: *ALAS1* is the ubiquitously  
480 expressed one while *ALAS2* expression is restricted to erythroid cells.  
481 Negative feedback regulation of *ALAS1* by heme has been reported and  
482 will be discussed later. Ferrochelatase (FECH) catalyses the last step of  
483 heme biosynthesis, namely the insertion of iron into PPIX. Heme bio-  
484 synthesis has been extensively reviewed elsewhere [52,55,69].

#### 485 4.2. Can sideroflexins regulate iron homeostasis ?

486 The first evidence for a link between sideroflexins and iron metabo-  
487 lism came from a study of the *flexed-tail* mouse, which harbors a muta-  
488 tion in a locus containing the *Sfxn1* gene [1]. Mice mutant for *Sfxn1*  
489 displayed sideroblastic anemia, microcytic anemia and hypochromic  
490 erythrocytes. Furthermore, *flexed-tail* mice were also displaying iron de-  
491 posits in the mitochondria from erythrocyte precursors. Nevertheless,  
492 no mechanisms regarding the iron accumulation in the mitochondria  
493 were proposed; but since then, sideroflexins were annotated as proteins  
494 implicated in iron metabolism.

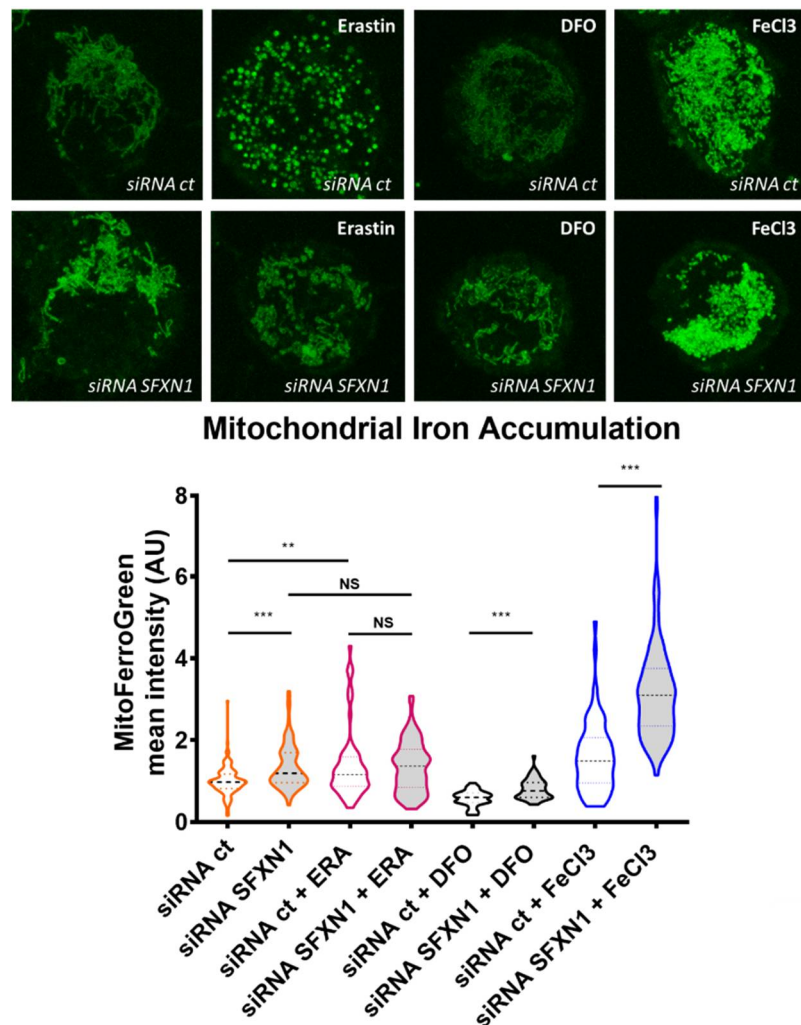
495 Based on the annotation of SFXN as transporters of metabolites re-  
496 quired for iron metabolism, we and others have tried to monitor the  
497 consequences of the loss of SFXN on iron cellular levels. **Table 3** sum-  
498 marizes the experimental evidence for an iron imbalance in the absence  
499 of SFXN. Whereas Mon *et al.* reported increased mitochondrial iron lev-  
500 els in HEK SFXN2 KO cells [9], an ICP-MS analysis did not show sig-  
501 nificantly modified cellular or mitochondrial iron levels in HEK *SFXN1*



502 KO cells compared to parental cells but an increase in cellular  $Mn^{2+}$  [15].  
503 Of note, albeit not significant, it seems that the loss of SFXN1 also  
504 slightly enhanced mitochondrial iron levels measured by ICP-MS, with  
505 a more pronounced effect in one of the two SFXN1-KO clones [15].  
506 Maybe, a significant increase could have been seen with more replicates  
507 or by quantifying mitochondrial iron by a TEM-EDX analysis as done  
508 for SFXN4 KO cells [31]. Despite an appropriate methodology, caution  
509 must also be taken when analyzing the results obtained by Mon *et al*  
510 because this study was done with only one cellular clone obtained after  
511 CRISPR/Cas9 invalidation of the *SFXN2* gene. However, expression of  
512 a SFXN2-mCherry fusion protein restored basal mitochondrial  $Fe^{2+}$  lev-  
513 els in these SFXN2 KO cells, as measured with a specific fluorescent  
514 probe. Loss of SFXN4 was also proven to alter iron levels in the K562  
515 leukemic human cell line. Whereas labile cytosolic iron pool was de-  
516 creased, Paul *et al.* have provided evidence for a redistribution of cellu-  
517 lar iron from the cytosol to the mitochondria in K562 *SFXN4* KO cells  
518 [31].

519 In our lab, we are interested in the early events triggered by the  
520 depletion of SFXN1 in mammalian cells. To investigate the effect of a  
521 decrease in SFXN1 protein levels, we chose to transiently deplete  
522 SFXN1 in HT1080 human cells using siRNA and then, we quantified  
523 mitochondrial labile Fe(II) levels using the MitoFerro-Green probe [70].  
524 Depleting SFXN1 in HT1080 cells induced a slight but reproducible in-  
525 crease in mitochondrial iron levels as shown in **Figure 5**. This increase  
526 in mitochondrial Fe(II) when SFXN1 levels are lowered, could be either  
527 a consequence of a defective heme biosynthesis, since Fe(II) is the sub-  
528 strate of FECH that inserts it into protoporphyrin IX, or a consequence  
529 of the catabolism of heme by HO-1 (heme oxygenase-1). Additionally,  
530 our data enlighten an erastin-dependent increase in labile Fe(II) mito-  
531 chondrial levels in HT1080 cells. A similar increase was also reported  
532 in erastin-treated MEF cells [71]. In HT1080 and MEF cells, erastin was  
533 previously shown to induce HO-1 expression [72,71], which may ex-  
534 plain the increase in mitochondrial Fe(II) that we observed in erastin-  
535 treated H1080 cells. Whether reducing SFXN1 levels inhibits FECH ac-  
536 tivity or promotes heme catabolism must be further investigated.

537 Altogether, the evidence enounced above point towards a role for  
538 SFXN in the maintenance of appropriate iron levels since the depletion  
539 or loss of SFXN1, SFXN2 and SFXN4 may increase mitochondrial iron  
540 by mechanisms that remain unknown. Mitoferrin1 and Mitoferrin2 are  
541 known as iron importers into the mitochondria and ABCB8 as an iron  
542 exporter [73]. Thus, due to the fact that iron mitochondrial transporters  
543 have been already described, and that the lack of either SFXN 1, 2 or 4  
544 leads to intramitochondrial iron accumulation, we do not favor the pos-  
545 sibility that SFXN are iron transporters. So, other intriguing possibili-  
546 ties should be explored.



547  
548  
549  
550  
551  
552  
553  
554  
555  
556  
557  
558  
559  
560  
561  
562  
563  
564  
565  
566  
567  
568

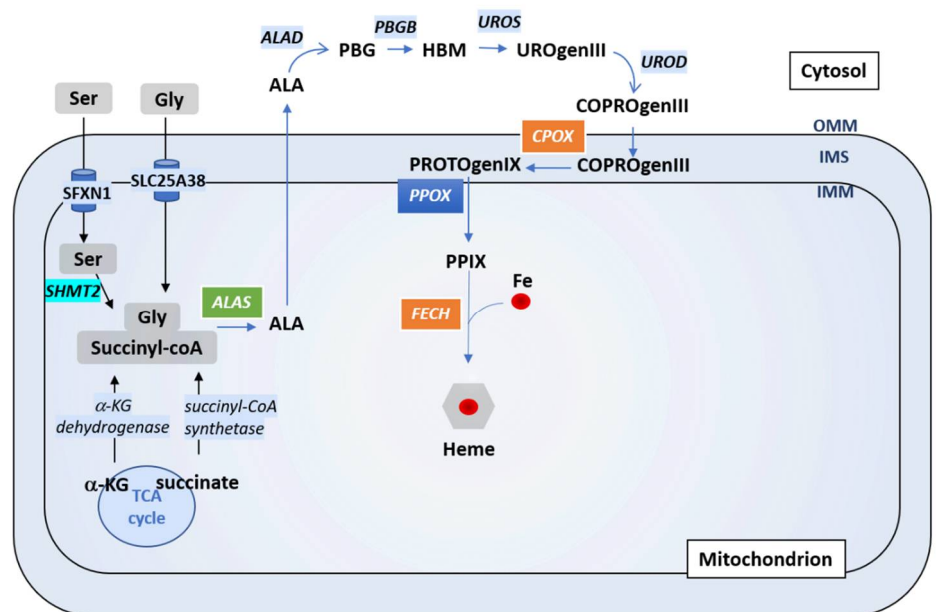
**Figure 5. Depleting SFXN1 in HT1080 human cells leads to an intramitochondrial iron accumulation.** *Top panel:* mitochondrial labile Fe(II) staining using the MitoFerro-Green probe [70] after transient transfection with a control siRNA (siRNA ct) or a pool of SFXN1-targeting siRNA (siRNA SFXN1). Cells were further treated with DMSO (vehicle), erastin, DFO or FeCl<sub>3</sub>. Erastin is a drug that is widely used to trigger ferroptosis, DFO (deferoxamine) is an iron chelator that lowers mitochondrial iron levels and is used as a negative control. FeCl<sub>3</sub> increases intracellular iron levels and served as a positive control. SFXN1 depleted cells show higher mitochondrial iron levels than control cells (siRNA scramble transfected cells). Erastin promotes iron accumulation. In control cells (siRNA ct), erastin increases mitochondrial iron levels and a punctuate staining is seen, maybe revealing mitochondrial network fission. In SFXN1 depleted cells, erastin does not seem to further increase mitochondrial iron levels. In all conditions except with erastin, iron levels are increased after SFXN1 depletion, compared to control, suggesting that erastin and SFXN1 could use the same mechanisms to lead to an increase in mitochondrial iron. Same magnification is used for all images. *Bottom panel:* quantification of three independent assays (n>50 cells per condition) in which fluorescent signal is measured and values are normalized to siRNA ct mean levels (mean =1). After Mann-Whitney tests, significant differences are shown (\*\* p<0.01, \*\*\* p>0.001, NS Not Significant). See Appendix A.2 for experimental details.

569  
570  
571  
572

Proper iron homeostasis requires a fluid transport of iron and its derivatives through the mitochondrial membranes and the cytosol. In this regard, the ALA (Aminolevulinic acid) synthesis requires Gly import through SCL25A38 on the one hand, and ALA export on the other

573  
574  
575  
576  
577  
578  
579  
580  
581  
582  
583  
584  
585  
586  
587  
588  
589  
590

hand, presumably through the same transporter (**Figure 6**) [74]. SFXN1 was shown to be a Serine transporter *in vivo* [8]. Intramitochondrial Ser would be catabolized by SHMT2 into Gly and 5,10-meTHF (5,10 methyl tetrahydrofolate) to enter in the OCM pathway, necessary for purine synthesis, pointing out that SFXN1 could be linked to the first and limiting step of heme synthesis. Moreover, once protoporphyrin is generated in the intermembrane space, it must enter the mitochondrial matrix for the last heme synthesis step using both ABCB6 and ABCB10 transporters [75,76]. Anyway, it cannot be excluded that other sideroflexins could be involved in this event. Whether SFXN1 could bind to heme and help in its trafficking is another hypothesis that merits our attention. We thus seek for heme binding motifs (HBMs) in SFXN1 with the SeqD-HBM tool dedicated to the prediction of heme-coordination sites in protein sequences [77,78] and we found four HBMs that are solvent-accessible (**Figure S1, Appendix A**). These predicted HBM may permit transient interactions between heme and SFXN1. Biochemical studies are needed to confirmed these interactions and further investigate their significance regarding SFXN1 activity.



591  
592  
593  
594  
595  
596  
597  
598  
599  
600  
601  
602  
603

**Figure 6. Regulation of heme biosynthesis by SFXN1.** Gly and succinyl CoA are the substrates to generate ALA, the first heme precursor, thanks to ALAS enzyme. Gly can enter directly into the mitochondria by SLC25A38, or can be the result of Ser transformation (previously imported by SFXN1) by SHMT2. ALA is further exported to the cytosol where the next steps of heme biosynthesis are catalysed by ALAD, PBGB, UROS and UROD. CPOX, PPOX and FECH are the three mitochondrial enzymes that catalyze the three last steps of heme synthesis (see main text). The last step corresponds to the incorporation of iron into the protoporphyrin PPIX to complete the heme synthesis. Cells lacking SFXN1 show decreased CPOX and FECH mRNA and protein levels (orange box), but higher amount of ALAS protein (green box), according to Acoba *et al.* [15].

604  
605  
606  
607  
608

To conclude, several open questions are remaining about the role of SFXNs in iron homeostasis. For example, are SFXN3 and SFXN5, like SFXN1, 2 and 4, able to regulate iron levels? No studies have been performed in this regard yet. Do sideroflexins alter iron levels by regulating the activity of other regulators implicated in iron homeostasis?

609 How can we explain that low SFXN1 levels (as well as low levels of  
610 SFXN2 or 4) lead to an increase of mitochondrial iron, and that an in-  
611 crease in SFXN1 may also trigger an increase mitochondrial iron level  
612 (see section 5.2)? What are the relationships between iron homeostasis  
613 disturbance and one carbon metabolism? To answer those questions,  
614 further work in mammalian cells is needed, and later confirmed using  
615 *in vivo* models.

#### 616 4.3. Which role for sideroflexins in heme biosynthesis and ISC biosynthesis ?

617 Whether SFXN1 and its homologues can regulate heme biosynthe-  
618 sis has not been thoroughly investigated so far, but recent studies gave  
619 evidence for an impairment of heme biosynthesis when certain mem-  
620 bers of the SFXN family are lacking [9,15,31]. Interestingly, SFXN1 loss  
621 in human kidney embryonic cells was recently reported to impair heme  
622 biosynthesis [15]. Indeed, cells lacking SFXN1 showed reduced heme  
623 levels, decreased CPOX and FECH transcripts and protein levels but  
624 increased ALAS1 protein levels. It is well-known that heme can induce  
625 ALAS1 degradation by a mechanism involving, at least, ALAS1 bind-  
626 ing to the mitochondrial protease CplXP [79]. It is thus likely that low  
627 heme levels found in SFXN1 cells limits heme binding to ALAS1 and  
628 consequently inhibits its degradation by CplXP. These defects in heme  
629 biosynthesis may explain the less efficient mitochondrial respiration  
630 and, especially, Complex III loss of activity. Accordingly, whereas for-  
631 mate had no effect, hemin supplementation increased CIII activity in  
632 wild-type and *SFXN1* KO cells but only partially restored the assembly  
633 of CIII in *SFXN1* KO cells [15]. However, hemin was unable to restore  
634 basal levels of Complex III subunits in HEK *SFXN1* KO cells suggesting  
635 that other defects are present in these cells. Interestingly, DMK (dime-  
636 thyl-  $\alpha$ -KG, a cell permeant analogue of  $\alpha$ -KG) rescued almost totally  
637 CIII subunits levels and CIII activity in HEK *SFXN1* KO. Succinyl-coA  
638 that serves in the first step of heme biosynthesis can originate from  $\alpha$ -  
639 KG or succinate. Hence, in the mitochondrial matrix,  $\alpha$ -KG can be con-  
640 verted in succinyl-coA by  $\alpha$ -KG dehydrogenase, a highly regulated en-  
641 zyme of the TCA cycle [80]. It would thus be interesting to determine  
642 if, additionally to the decreased GDH and ALT activity observed in  
643 *SFXN1* null cells [15],  $\alpha$ -KGDH activity is also impaired upon the loss  
644 of *SFXN1*.  
645

**Table 3.** Regulation of systemic or cellular iron levels by SFXN.

| <i>Protein</i> | <i>Model</i>                   | <i>Evidence</i>                                                                                                            | <i>Methodology</i>                                                                    | <i>Reference</i>                                         |
|----------------|--------------------------------|----------------------------------------------------------------------------------------------------------------------------|---------------------------------------------------------------------------------------|----------------------------------------------------------|
| SFXN1          | Mouse                          | Iron overload in mitochondria of erythrocytes in the <i>flexed-tail</i> mouse                                              | Iron mitochondrial staining                                                           | Fleming <i>et al</i> , 2001<br>Acoba <i>et al</i> , 2020 |
| SFXN2          | HEK SFXN1 <sup>KO</sup> cells  | Increased mitochondrial iron                                                                                               | ICP-MS                                                                                | Mon <i>et al</i> , 2019                                  |
|                | HEK SFXN2 <sup>KO</sup> cells  | Increased mitochondrial iron levels                                                                                        | ICP-MS<br>MitoFerro-Green staining and confocal microscopy                            |                                                          |
| SFXN3          | Mouse Sfnx3 KO                 | Decreased circulating iron levels in male transgenic mice homozygous for the <i>Sfnx3</i> <sup>tm1b(KOMP)Wtsi</sup> allele | Biochemical assay                                                                     | The IMPC database <sup>2</sup>                           |
| SFXN4          | K562 SFXN4 <sup>KO</sup> cells | Decreased labile iron pool                                                                                                 | Indirect biochemical measure based on the dequenching of calcein upon release of iron | Paul <i>et al</i> , 2019                                 |
| SFXN5          | -                              | Increased mitochondrial iron levels                                                                                        | TEM-EDX                                                                               |                                                          |
|                |                                | -                                                                                                                          | -                                                                                     | -                                                        |

<sup>1</sup> ICP-MS is for inductively coupled plasma atomic emission - mass spectrometry, TEM-EDX is for Transmission electron microscopy-Energy dispersive X-Ray analysis. <sup>2</sup> website page for SFXN3 : <https://www.mousephenotype.org/data/genes/MGI:2137679#phenotypesTab>.

646

647

648

649

650 Impairment of heme biosynthesis upon SFXN loss could be explained by the function  
651 of serine transporter attributed to SFXN. Following its import into the mitochondrion, Ser  
652 can be converted in Gly and 5,10-me-THF involved in folate cycle and OCM. An imbalance  
653 in the cellular Ser/Gly ratio may impair heme biosynthesis since Gly is (with succinyl-  
654 coA) the precursor for the synthesis of protoporphyrins into which iron is incorporated in  
655 the final step of heme synthesis catalyzed by FECH (**Figure 6**). As SFXN1 is presumed to  
656 be the mitochondrial transporter of Ser, its loss could increase cellular Ser and lower Gly  
657 levels. Indeed, in Jurkat and K562 SFXN1 KO cells, the cellular Ser/Gly ratio was increased  
658 and associated to increased cellular Ser levels but decreased Gly levels [8]. In agreement  
659 with an imbalance in serine levels upon SFXN1 loss, HEK SFXN1 KO cells also have in-  
660 creased cellular Ser levels and Ser/Gly ratio but no decrease in Gly cellular levels were  
661 reported [15]. Whether this discrepancy can be explained by a cell type specificity or other  
662 reason remains to be elucidated. Of note, mitochondrial levels of those two amino acids  
663 have not been assessed and it will be interesting to more specifically address the presence  
664 of Ser and Gly inside the mitochondrion by a metabolomics study on this organelle.

665 SFXN2 has been recently described in HEK293 cells to have a key role in iron metabo-  
666 lism, mainly in heme synthesis [9]. High levels of iron have been shown in mitochondria  
667 in SFXN2 knockout HEK293 cells. Also, a decreased activity of Complexes II-IV but not of  
668 the Complex I was noticed. Complex I subunits contain Fe-S clusters, in contrast to Com-  
669 plex IV, which is mainly composed by heme groups. Complexes II and III contain both  
670 Fe-S clusters and heme groups (**Figure 2**). Thus, as no effect in Complex I was detected,  
671 and no decrease in Frataxin (FXN), a mitochondrial enzyme required for the Fe-S cluster  
672 formation, nor in ALAS2, the enzyme that catalyzes the first step of the heme biosynthetic  
673 pathway, was reported, it was concluded that SFXN2 mutants affected heme synthesis  
674 after the first step of heme biosynthesis, but not the Fe-S cluster formation. However, nei-  
675 ther the levels of ISC-containing proteins nor those of ALAS1 have been assessed in this  
676 study. It is surprising because ALAS2 is the erythroid specific form and ALAS1 the house-  
677 keeping one.

678 We propose few possibilities to explain SFXN2 knockout cells phenotype. The lack  
679 of SFXN2 could either lead to an impaired ALA export or no mitochondrial import of  
680 protoporphyrin (PPIX) for the last step of the heme pathway. A defective mitochondrial  
681 export of the heme groups is another plausible explanation. Finally, other options could  
682 be possible as an interaction of SFXN2 with BCS1L, a chaperone anchored to the inner  
683 mitochondrial membrane that is required for proper assembly of the Complex III (see sec-  
684 tion 2.2 for more details). In all those cases, an intramitochondrial iron accumulation is  
685 presumed. All those possibilities, and others, must be studied to be able to clarify the pos-  
686 sible role of Sfxn2 in heme biosynthesis.

#### 687 4.4. Which role for sideroflexins in ISC biosynthesis ?

688 Loss of SFXN also seems to impair ISC biogenesis. Indeed, in the absence of SFXN4  
689 there is a decrease in Fe-S cluster levels which is consistent with the decrease of Complex  
690 I activity seen in SFXN4 KO cells, pointing out that this SLC56 carrier could play a role in  
691 Fe-S biosynthesis [30,31]. As a consequence of the low Fe-S levels, IRP1 aconitase activity,  
692 as well as labile iron cytosolic levels, also decreases, whereas mitochondrial iron increases,  
693 suggesting that iron import in the mitochondria is not impaired, and instead possibly en-  
694 hanced. Those features are very similar to the lack of mitochondrial frataxin, which leads  
695 to Friedreich's Ataxia, also known as X-linked sideroblastic anemia. Frataxin (FXN) is a  
696 mitochondrial chaperone that interacts with aconitase in a citrate-dependent manner to  
697 convert (3Fe-4S)<sup>1+</sup> inactive enzyme into [4Fe-4S]<sup>2+</sup> active one within the Krebs cycle. It  
698 also interacts with the ISCU-NFS1 (Iron-Sulfur Cluster Scaffold-Cysteine desulfurase) in  
699 the final steps of Fe-S formation [81,82]. The reduction of mitochondrial aconitase (ACO2)  
700 in SFXN4 KO cells [31] suggests that SFXN4 could participate in the Fe-S biosynthesis  
701 maybe through an interaction with Frataxin (FXN). It has been previously reported that  
702 FECH, an important enzyme for heme biosynthesis, Mfrn1, an iron transporter into the  
703 mitochondria, and ABCB10, a protoporphyrin IX transporter, could form a complex in

704 mouse erythroleukemia (MEL) cells to direct iron incorporation into protoporphyrin to  
705 form heme [54,83]. Taken together, those results open the possibility that SFXN4 and FXN  
706 interact with other proteins such as aconitase or the ISCU-NFS1 multimeric complex to  
707 mature the Fe-S clusters. We have recently performed a screen with the aim to identify  
708 the direct partners of SFXN1 protein in MCF7 cells (Tifoun et al., in preparation) and, even  
709 though Sfxn1 does not interact directly with FXN, it is still possible that Sfxn4 could do  
710 so. In Sfxn4 mutants Fe-S synthesis is reduced, pointing out that Sfxn4 may play a role in  
711 the first steps of Fe-S cluster formation, maybe through FXN interaction. A recent study  
712 shows that the ISC (Iron Sulfur Cluster, composed by NFS1, ISCU and FXN) function re-  
713 quires L-Cysteine to generate de disulfide groups necessary to form the Fe-S clusters [84].  
714 Moreover, it has been postulated that SFXN1 could transport not only serine, but alanine  
715 and possibly also glycine and cysteine *in vitro* [8]. Actually, in SFXN1 depleted cells have  
716 a proliferative advantage in media containing low cystine (dimer of cysteine formed un-  
717 der oxidant conditions), this could be due to the fact that the amino acid cysteine is nec-  
718 essary for cytosolic glutathione synthesis and that a loss of mitochondrial import would  
719 increase its availability for those purposes [8]. The lack of SFXN1 activity can be overcome  
720 by SFXN2 and SFXN3 but not by SFXN4 [8]. SFXN4 cannot substitute SFXN1 for Ser im-  
721 port into the mitochondria, but it could maybe have a higher affinity for Cys. This may  
722 explain why SFXN1 and SFXN2 mutants present mainly problems in heme synthesis  
723 whereas SFXN4 KO cells have deficiencies in Fe-S cluster formation, as Ser and Gly are  
724 essential for the ALA synthesis and Cys is required for proper Fe-S maturation.

725 How could SFXN regulate iron levels and heme biosynthesis remains unanswered  
726 and whether SFXN impair mitochondrial iron and heme homeostasis by direct or indirect  
727 actions is unknown. We have recently documented the interaction between SFXN1 and  
728 ATAD-3 (Tifoun *et al*, in preparation). Because *Caenorhabditis elegans* ATAD-3 was shown  
729 to modulate mitochondrial iron and heme homeostasis, heme biosynthesis regulation by  
730 SFXN1 may depend on its interaction with ATAD-3. Interestingly in *atad-3* (RNAi) worms,  
731 mitochondrial but not cytosolic iron levels were increased and an altered expression of  
732 iron homeostasis genes was reported [85]. Indeed *atad-3* knockdown (KD) led to an in-  
733 crease in *ftn-1* but a decrease in *ftn-2* mRNA (respectively encoding the intestinal ferritin  
734 heavy chain and a more ubiquitous one). *aco-1* (encoding the homologue of the mammalian  
735 IRP responsible of the post-translational regulation of ferritin), *fpn-1.1* (encoding a *C. ele-*  
736 *gans ferroportin* homologue) and *smf-3* mRNA (involved in the cellular uptake of non-heme iron)  
737 were reduced. Expression of *mfn-1* (the sole Mitoferrin encoding gene in *C. elegans*) was un-  
738 changed upon *atad-3* knockdown. In agreement with a mitochondrial iron overload, *atad-3* KD in  
739 worms also led to an accumulation of Hemin (a heme-containing protein involved in erythroid  
740 differentiation) and a fluorescent analogue of heme.

741 Interestingly, a new mutation of ATAD3A (Arg528Trp), which has been described in  
742 7 families [86], is responsible of developmental delay, hypotonia, optic atrophy, axonal  
743 neuropathy and hypertrophic cardiomyopathy. In some of those individuals, a deficiency  
744 of complex III and citrate synthase was detected. Those results look similar to the conse-  
745 quences of the lack of SFXN1 or SFXN4 proteins. ATAD3A, being a transmembrane pro-  
746 tein that binds both external and internal mitochondrial membranes, could interact with  
747 SFXN1 and/or SFXN4 to control iron metabolism. Moreover, the use of *Drosophila* in this  
748 study, allowed to see that either lack of *bor* (*belphegor*, ATAD3A homologue), either the  
749 expression of a R534W form, a variant of Arg528Trp human ATAD3A, in the larval neu-  
750 romuscular junctions (NMJ) promoted a decreased of mitochondrial content, aberrant mi-  
751 tochondrial morphology and increased autophagy. Complementary, *bor* overexpression  
752 promoted larger and elongated mitochondria in the NMJ. Whether SFXN family has a role  
753 in autophagy remains completely unexplored and merits attention.

## 754 5. Sideroflexins, ferroptosis and ferritinophagy

### 755 5.1. SFXN, cell death and ferroptosis

756 Growing evidence support the key role of iron metabolism in ferroptosis, even if the  
757 exact mechanisms are not fully elucidated [87]. Ferroptosis is a physiological cell death  
758 contributing to tissue homeostasis and implicated in pathology (cancer, neurodegenerative  
759 disease and cardiac injury). Mechanistically, ferroptosis is an iron-dependent but  
760 caspase-independent regulated cell death (RCD) triggered by uncontrolled lipid peroxi-  
761 dation leading to dramatic morphological changes in mitochondria. For recent reviews on  
762 the place of mitochondria in ferroptosis regulation, the reader is invited to refer to [88,89].  
763 Ferroptosis can be triggered by diverse drugs such as erastin, RSL3 or FIN56, among many  
764 others, and this type of RCD is prevented by iron chelators and antioxidants [90]. The  
765 mitochondrion appears as a main contributor to ferroptosis because of its central place in  
766 iron metabolism and the fact that several mitochondrial metabolic pathways – including  
767 TCA cycle, and ETC - contribute to PL-PUFA (polyunsaturated fatty acid containing  
768 membrane phospholipids) peroxidation.

769 Few data are available on the role of SFXN in cell death and ferroptosis regulation.  
770 *SFXN4* gene knockout was reported to promote cell death of K562 human cells in galac-  
771 tose-containing medium, together with an increase in caspase 3/7 activity [31]. Whether  
772 the loss of *SFXN4* triggers ferroptosis was not investigated to our knowledge. Interest-  
773 ingly, in HEK kidney embryonic cells, *SFXN2* gene knockout seems to sensitize cells to  
774 erastin-induced cell death however, the underlying mechanisms were not deeply investi-  
775 gated [9].

776 Recently, *SFXN1* was showed to participate in LPS-induced ferroptosis in H9c2 car-  
777 diomyocytes, a process depending of NCOA4-mediated ferritinophagy [91]. Li *et al*  
778 showed an LPS- and NCOA4-dependent upregulation of *SFXN1* and documented the role  
779 of *SFXN1* in LPS-induced ferroptosis. Briefly, in LPS-treated H9c2 cardiomyocytes cells,  
780 knockdown of *SFXN1* increased cell viability, restored intramitochondrial basal levels, in-  
781 hibited mitochondrial ROS production, decreased lipid peroxidation and levels of PTGS2  
782 (also known as cyclooxygenase-2) and MDA. Collectively, these data suggest that *SFXN1*  
783 promotes LPS-induced ferroptosis, however the molecular mechanisms are far from being  
784 clear. Li *et al* explained this role by *SFXN* implication in the iron mitochondrial import,  
785 which has not been proven yet. Further work is thus needed to investigate the relation-  
786 ships between *SFXN1* and ferroptosis, and the precise mechanisms whereby *SFXN1* could  
787 regulate iron levels and cell death. It will be also interesting to determine if *SFXN1* medi-  
788 ates LPS-induced ferroptosis in other cell types, as well as its implication in ferroptosis  
789 mediated by different inducers (such as erastin, RSL3, FIN56 or other drugs). Because  
790 Acoba *et al.* reported lowered CoQ levels in *SFXN1* KO cells and CoQ is an antioxidant  
791 and a cofactor for the ferroptosis suppressor FSP1 [92], we expect that an imbalance in  
792 *SFXN1* levels may favor ferroptosis through a direct or indirect regulation of CoQ levels.  
793 It would thus be interesting to study FSP1 activity in *SFXN1* KO cells.

## 794 5.2. *SFXN1* and ferritinophagy

795 To limit the toxicity of free  $Fe^{2+}$ , molecular traps – *e.g* Ferritin and FtMt (mitochondrial  
796 ferritin) - exist in the cytosol and the mitochondrion respectively, as stated earlier. Ferri-  
797 tinophagy, the lysosome-dependent mechanism whereby iron is mobilized from ferritin,  
798 can also contribute to ferroptosis induction. In this process, the selective cargo receptor  
799 NCOA4 (nuclear receptor coactivator 4A) binds to ferritin and targets this iron storage  
800 protein to the lysosomes, thus promoting ferritin degradation and the subsequent release  
801 of iron [93]. In apelin-13 induced cardiomyocytes hypertrophy, Tang *et al* recently re-  
802 ported a decrease in FTH (ferritin heavy chain) together with an upregulation of NCOA4  
803 and *SFXN1* [94]. Immunohistochemical analysis of hypertrophic heart tissue also high-  
804 lighted an upregulation of NCOA4 and *SFXN1*. The siRNA-mediated depletion of  
805 NCOA4 restored basal levels of *SFXN1* in cardiomyocytes, suggesting that apelin-13 me-  
806 diated upregulation of *SFXN1* could depend on NCOA4. In the presence of apelin-13, the  
807 knockdown of *SFXN1* decreased iron overload and mitochondrial ROS production in fer-  
808 ric ammonium citrate – treated cardiomyocytes. How NCOA4 could upregulate *SFXN1*

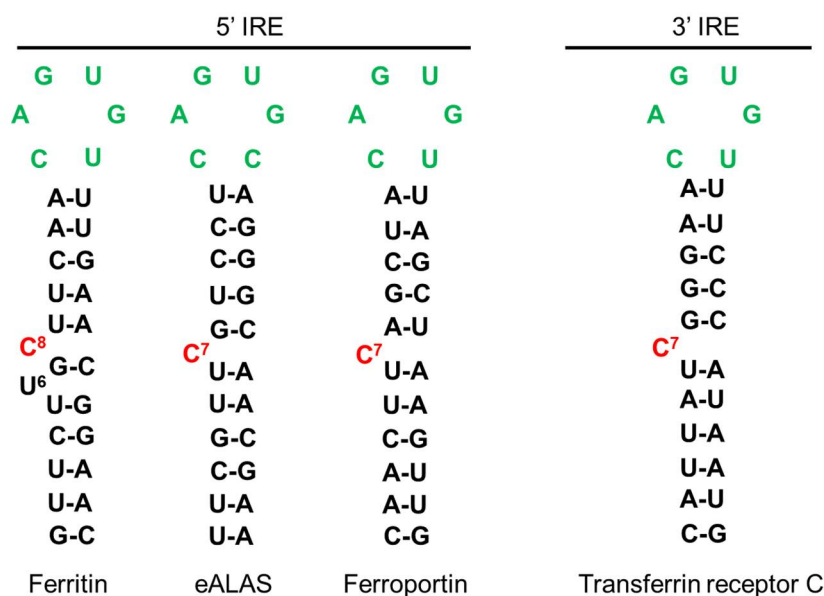


809 remains unanswered, as well as the role of SFXN1 and the other SFXN/SLC56 transporters  
810 in cardiac hypertrophy. In this study, SFXN1 is proposed to be an iron importer, together  
811 with mitoferrin 1 and 2, which are upregulated. The increase of mitochondrial iron in the  
812 induced cardiomyocytes hypertrophy model responds to the elevated SFXN1 levels, and  
813 higher amounts of iron would promote ROS production thanks to the Fenton reaction, an  
814 increase of lipids peroxidation and finally, an induction of ferroptosis. Nevertheless, the  
815 mechanisms that allow SFXN1 to control iron levels are not addressed nor whether SFXN1  
816 is the most important player in regulating mitochondrial iron, aside of mitoferrins and  
817 ferritin, is discussed.

818 NCOA4 mediated regulation of SFXN1 was also reported in a recent study address-  
819 ing the role of ferritinophagy in sepsis-induced cardiac injury [91]. In this study, SFXN1  
820 was shown to be upregulated at the mRNA level in LPS-treated cardiomyocytes, but  
821 whether this upregulation results from a transcriptional activation or an enhanced stabil-  
822 ity of mRNA was not studied. To date, the regulation of SFXN expression has not been  
823 deeply investigated and further work is needed to document this point. However, intra-  
824 cellular iron may be important for NCOA4-mediated SFXN1 regulation since the iron che-  
825 lator deferoxamine (DFO) was shown to decrease LPS-induced SFXN1 accumulation [91].  
826 Li *et al* used immunofluorescence to show this DFO-mediated downregulation of SFXN1  
827 and this must be confirmed using western blot.

828 The iron-mediated regulation of SFXN1 levels is intriguing and we wondered if iron  
829 could regulate translation or mRNA stability by IRP-dependent molecular mechanisms.  
830 We hypothesize that IRP proteins, that are major regulators of iron homeostasis acting at  
831 the post-transcriptional levels, could modulate SFXN levels through binding to cis-regu-  
832 latory IRE response elements in SFXN1 transcripts. We thus searched for IRP-binding sites  
833 in SFXN transcripts. IRE found in some of the iron-regulated transcripts are shown in  
834 **Figure 7**. Canonical IRE are motifs composed of a six-nucleotide apical loop (5'-CAG-  
835 WGH-3') [95]. Using an IRE prediction tool ("SIREs Web Server 2.0"  
836 (<http://ccb.g.imppc.org/sires/>) [96], we retrieved putative IRE in all human SFXN1 variant  
837 transcripts except for one (**Table 4**). One IRE of high quality and a second one of low  
838 quality are found respectively at the end of the SFXN1 coding sequence and in the 3' UTR  
839 (**Figure 8**). Additionally, human SFXN2 transcripts possess one putative medium-quality  
840 IRE and SFXN5 transcripts contain a putative high-quality IRE, at their 3' UTR. Interest-  
841 ingly, no IREs are predicted neither in SFXN3 nor in SFXN4 mRNAs. As SFXN1 and  
842 SFXN3 are closely related and seem to have highly similar three-dimensional structure, it  
843 is tempting to hypothesize that they can be differentially regulated depending on iron  
844 levels. In *Drosophila*, no putative IREs are predicted in any of the two mRNAs encoding  
845 dSfxn1/3 and dSfxn2, the SFXN orthologues found in flies. The presence of putative IREs  
846 at the 3'UTR of some of SFXN transcripts is suggestive of their IRP-mediated stabilization.  
847 We thus expect an increase of SFXN1 levels under low iron levels, when IRP1 lacks its Fe-  
848 S cluster and IRP2 is degraded. This latter is not in agreement with the DFO-mediated  
849 downregulation of SFXN1 levels reported by Li *et al* [91]. IRE motifs found in SFXN tran-  
850 scripts are non-canonical IRE motifs derived from IRE sequences identified in IRP-inter-  
851 acting mRNAs uncovered in the genome-wide SELEX experiments [97–99]. Having found  
852 IRE in SFXN1 transcripts is in favor of an iron-mediated regulation of SFXN levels, how-  
853 ever, whether the IREs found in SFXN1, SFXN2 and SFXN5 transcripts are functional, is a  
854 point that needs to be further investigated.

855 To conclude, despite two works started to shed light on SFXN1 role in iron homeo-  
856 stasis and ferroptosis [94,91], how this metabolite transporter exerts its function is far from  
857 being clear and more work is required to properly elucidate mechanistically how SFXN1  
858 is implicated in iron homeostasis.



859

860

861

862

863

864

865

866

867

**Figure 7. IRE sequences from known proteins involved in iron metabolism.** IRE sequences can be localized at 5' or 3'. In the absence of iron, IRP1 binds the sequences located at 5' of blocking the translation of the RNA. Ferritin, ALAS and Ferroportin are proteins involved in iron storage, heme synthesis and iron export, respectively. In the same situation, IRP binding to 3' sequences, stabilizes the RNA promoting the translation of, for example, Transferrin receptor, involved in iron import. In the opposite situation, with high iron levels, IRP binds to iron, which unbinds the IREs, thus promoting translation of Ferritin, ALAS and Ferroportin and leading to Transferrin receptor RNA decay, which is no more protected by IRP1.

868

**Table 4.** Location of predicted IRE in SFXN1 splicing variants.

| Sequence ID                                                                    | mRNA length | CDS position | Product                  | IRE position |           |
|--------------------------------------------------------------------------------|-------------|--------------|--------------------------|--------------|-----------|
| NM_022754.7 Homo sapiens sideroflexin 1 (SFXN1), transcript variant 1, mRNA    | 4066        | 90-1058      | sideroflexin-1 isoform 1 | 1000-1031    | 2698-2729 |
| NM_001322977.2 Homo sapiens sideroflexin 1 (SFXN1), transcript variant 2, mRNA | 4094        | 118-1086     | sideroflexin-1 isoform 1 | 1028-1059    | 2726-2757 |
| NM_001322978.2 Homo sapiens sideroflexin 1 (SFXN1), transcript variant 3, mRNA | 4037        | 244-1029     | sideroflexin-1 isoform 2 | 971-1002     | 2669-2700 |
| NM_001322980.2 Homo sapiens sideroflexin 1 (SFXN1), transcript variant 4, mRNA | 3938        | 90-875       | sideroflexin-1 isoform 4 | 872-903      | 2570-2601 |
| NM_001322981.2 Homo sapiens sideroflexin 1 (SFXN1), transcript variant 5, mRNA | 3966        | 118-903      | sideroflexin-1 isoform 4 | 900-931      | 2598-2629 |
| NM_001322982.2 Homo sapiens sideroflexin 1 (SFXN1), transcript variant 6, mRNA | 4065        | 272-1057     | sideroflexin-1 isoform 2 | 999-1030     | 2697-2728 |
| NM_001322983.2 Homo sapiens sideroflexin 1 (SFXN1), transcript variant 7, mRNA | 959         | 90-818       | sideroflexin-1 isoform 3 | No IRE       |           |

869

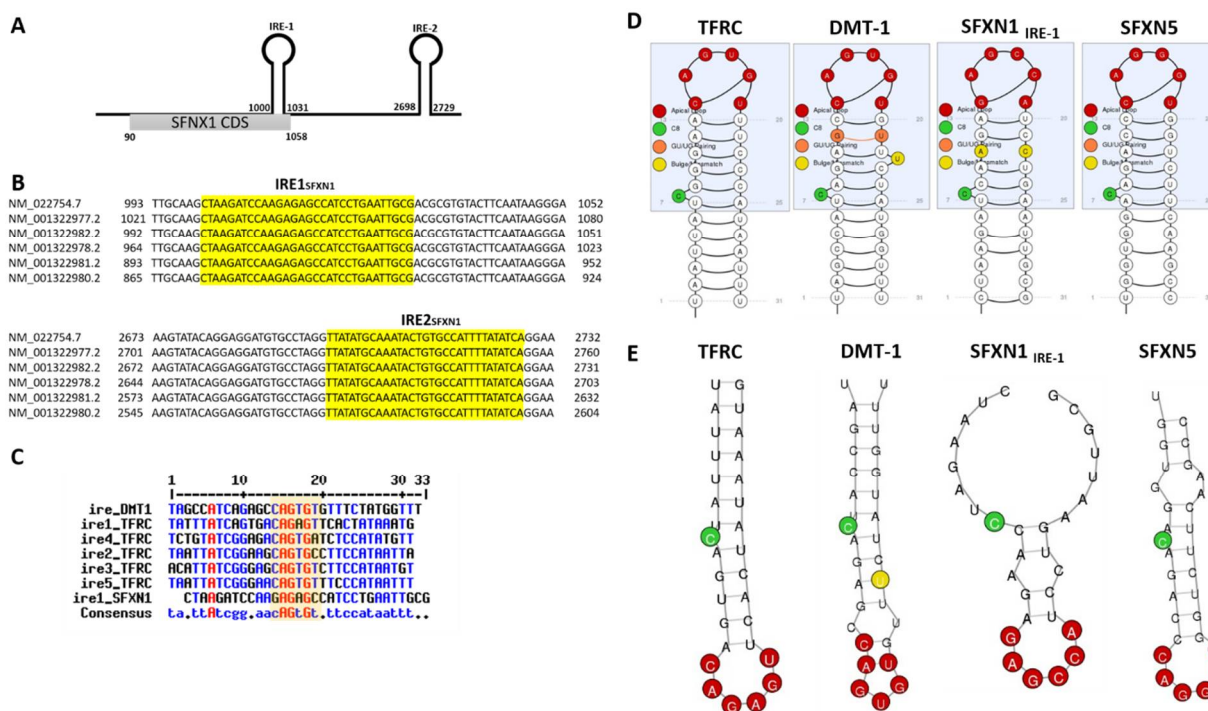


**Figure 8. Predicted IRE in SFXN transcripts.** A. Two IREs were found in the 3'UTR of SFXN1 transcripts using the SIREs Web Server 2.0. The first one is located at the end of the coding sequence. B. Alignment showing the position of the two IREs in SFXN1 transcripts. All except one shorter SFXN1 transcript variant possess putative IREs. C. Alignment of the IREs of DMT-1, transferrin receptor (TFRC) and SFXN1 transcripts using MultiAlin. The consensus highlights the position of the six-nucleotide apical loop (5'-CAGWGH-3') as shown in the yellow box. D, E. Schemes (D) and RNA fold prediction (E) for the IREs from TFRC, DMT-1, SFXN1 and SFXN5 transcripts generated by the SIREs Web Server 2.0.

## 6. Sideroflexins in aging: may SFXN regulate neuronal physiology and retinal function?

In this part, we discuss the potential role of SFXN in neuronal pathophysiology, aging and retinal function.

### 6.1. Sideroflexins and biometals in neuronal physiopathology

Brain accumulation of biometals - including iron and manganese - has been observed in neurodegenerative diseases and associated with a decline in cognitive functions [100–102]. Accumulation of biometals can be detrimental and may promote protein aggregation. Hence, Amyloid beta peptide (Aβ), which forms toxic aggregates in the brain of patients who suffered from Alzheimer's disease, is known to interact with iron [103–106]. Aβ toxicity was reported to be suppressed by the iron storage protein Ferritin in *Drosophila* [107].

We postulate that some SFXN may share a neuroprotective role because SFXN are present in brain neurons (Human Protein Atlas, [27] and our unpublished data) and a decreased expression of SFXN1 and SFXN3 was linked to Alzheimer's and Parkinson's diseases (AD and PD). Indeed, SFXN1 is decreased in brains of AD patients [108] and SFXN3 downregulated in late stage PD dopamine neurons from *substantia nigra* [109]. Additionally, downregulation of the *Drosophila* orthologue dSfxn1/3 enhanced tau toxicity in a *Drosophila* model commonly used to study neurodegeneration [108]. Under physiological conditions, SFXN3 and alpha-synuclein (α-Syn, a PD marker protein) levels were inversely correlated in a murine model, whereas overexpressing dSfxn1/3 impaired synapse morphology at the *Drosophila* neuromuscular junction [45]. It is tempting to link a putative iron-dependent regulation of SFXN, as discussed above, and the known regulation of α-Syn by IRPs. Hence, an IRE is found in the 5'UTR of α-Syn mRNAs and IRP-mediated translational inhibition is relieved upon high iron levels [58,110]. This could explain the

902 opposite regulation of  $\alpha$ -Syn and SFXN levels. However, we did not find putative IRE in  
903 SFXN3 transcripts, as stated above.

904 Decreased levels of SFXN1 in the hippocampus were also observed in a rat model  
905 with bilateral ovariectomy displaying depressive behaviors and cognitive impairment  
906 [111]. Recent evidence point towards a regulatory role for SFXN in iron homeostasis / uti-  
907 lization at the cell level [9,112,15]. However, iron homeostasis and heme biosynthesis have  
908 not been investigated specifically in SFXN-deficient neurons yet, and it would be interest-  
909 ing to question this point. Besides the mitochondrial accumulation of iron reported when  
910 some SFXN are lacking, Acoba *et al* also reported a decrease in manganese levels in  
911 SFXN1-null cells [15]. Manganese is an essential metal element required for the activity of  
912 certain enzymes (such as MnSOD) and both insufficiency and overexposure can affect  
913 neuronal physiology and cognitive functions [113]. Thus, SFXN might regulate neuronal  
914 physiology in participating in biometals homeostasis.

915 Whether SFXN are able to regulate ferroptosis is also an important concern, because  
916 ferroptosis is one of the most important regulated cell death in brain [114]. Ferroptosis  
917 was reported in Parkinson's disease, Alzheimer's disease and Huntington's disease and  
918 other neurologic disorders. Using *in vitro*, *ex vivo* and *in vivo* (mouse) PD models, Do Van  
919 *et al.* [115] reported ferroptosis in PD dopaminergic neurons, a process that was reversed  
920 by Ferrostatin-1, a selective inhibitor of erastin-induced ferroptosis which inhibits lipid  
921 ROS. Growing evidence also highlight the implication of ferroptosis in Alzheimer's dis-  
922 ease [116], a neurodegenerative disease characterized by cognitive functions and memory  
923 impairment, synaptic loss and neuronal cell death. In mouse, conditional deletion in fore-  
924 brain neurons of glutathione peroxidase 4 (Gpx4) gene altered cognitive functions (spatial  
925 learning and memory) and triggered hippocampal neurodegeneration with hallmarks of  
926 ferroptosis [117].

927 To conclude, further investigations must be undertaken to precisely specify the role  
928 of SFXN1 and its homologues in brain biometals homeostasis and neurodegeneration.

## 929 6.2. *Sfxn* and retinal degeneration

930 Iron levels vary during retina development, with gender and it accumulates during  
931 aging. When supply does not equal demand (*e.g.* if retinal blood flow is impaired), retinal  
932 neurons are at risk of excitotoxic cell death and vision is impaired or lost [118,119].

933 Many proteins are involved in iron homeostasis in the retina, and most of the rodent  
934 models studied, are related to human pathologies, like human atransferrinemia (lack of  
935 transferrin), hemochromatosis type IV (lack of ferroportin) or microcytic hypochromic  
936 anemia with iron overload (decrease in DMT1), among others (see [119] for a review).  
937 Human transferrin electrotransfection in rodents was shown to protect retinal structure  
938 and function, reducing microglial infiltration and preserving the integrity of the outer ret-  
939 inal barrier in a photo-oxidative model. Transferrin, a natural iron chelator, delayed also  
940 the retina degeneration and decreased oxidative stress [120]. This work validates iron  
941 overload as a therapeutic target for pathologies as retinitis pigmentosa or age-related mac-  
942 ular degeneration. Taking into account the relationships between SFXN and iron metabo-  
943 lism, we expect that the loss of SFXN could impair retinal function. Accordingly, in mice,  
944 *Sfxn3* mutations lead to retinal degeneration [121]. Using forward genetics and screening  
945 by optical coherence tomography, Chen *et al.* identified the *pew* and *basilica* mutations in  
946 the *Sfxn3* gene leading to a significant decrease in the outer retina thickness. Mice with  
947 CRISPR-Cas9-induced *Sfxn3* loss-of-function mutations were further generated to inves-  
948 tigate the consequences on retinal structure and function. Mice with predicted dramati-  
949 cally shortened *Sfxn3* proteins showed retinal impaired morphology (decreased retinal  
950 thickness, especially that of the outer retina, and loss of the hexagonal shape of retinal  
951 pigmentary epithelium cells) and abnormal fundus and vasculature compared to controls.  
952 Retinal thickness even decreased with age in favor of a retinal degeneration due to the  
953 lack of functional *Sfxn3*. Whether those defects are associated to impairment in iron ho-

meostasis is not explored nor discussed. Anyway, we favor the idea that SFXN3 contributes to regulate intracellular iron levels, thus protecting the retina from oxidative stress. Moreover, in humans, SFXN4 loss-of-function is associated with optic atrophy [19,21], pointing to SFXNs as a central family of proteins required for proper retina development and homeostasis.

## 7. Conclusion and open questions

SFXN/SLC56 is a new family of mitochondrial proteins that have important roles in amino acid transport and in iron homeostasis. Several studies associate SFXN depletion with an increase in mitochondrial iron, deficiencies in carbon metabolism and RC activity and ferroptosis, in cell culture, in animal models and in human pathology, making the SFXN an interesting target for tissue degeneration therapy. But even though those links seem clear and reproducible, nothing is known about the mechanism of action of SFXN. Do all the isoforms have the same functions (different members are expressed in different tissues)? As there are several transcripts for each isoform, do those different transcripts generate different proteins with different kinetic properties? If SFXN are not iron transporters, how can they control iron levels in the mitochondria? How can they control mRNA and/or protein levels of some key heme regulators (CPOX, FECH and ALAS)? Some SFXN present putative IRE but other don't; are all SFXN sensible to iron content and to IRP1/2 regulation?

We think that a better knowledge on SFXN biochemistry is needed to properly decipher the functions of each SFXN member, to know whether they all have redundant functions, their interaction with other proteins or with other SFXN, and how they are regulated.

## Abbreviations

ABC6: ATP Binding Cassette Subfamily B Member, ACO1: Aconitase1, AD: Alzheimer's disease,  $\alpha$ -KG:  $\alpha$ -ketoglutarate,  $\alpha$ -KGDH:  $\alpha$ -ketoglutarate deshydrogenase, AGK2 AcylGlycerol Kinase, ALA: Aminolevulinic acid, ALAD: Aminolevulinic acid deshydratase, ALAS: Aminolevulinic acid synthase, ALT2: Alanine aminotransferase 2, ICP-MS: Inductively coupled mass spectrometry, a-Syn: Alpha-synuclein, ATAD-3: ATPase family 3A domain containing protein, A $\beta$ : Amyloid beta peptide, BBG-TCC: Brain Bergmann Glial cell-Tricarboxylate carrier, BCS1L: Ubiquinol-Cytochrome C Reductase Complex Chaperone, BMP: Bone Morphogenetic Protein, CCHL: Cytochrome c heme lyase, COPROgenIII: Coproporphyrinogen III, CoQ: Coenzyme Q, COX4: Cytochrome c oxidase subunit 4, COXPD18: Combined oxidative phosphorylation deficiency 18, CPOX: Coproporphyrinogen oxidase, CYP450: Cytochrome P450, Cyt b: Cytochrome b, Cyt c1: Cytochrome c1, DFO: Deferoxamine, DMK: dimethyl- $\alpha$ -ketoglutarate, DMSO: Dimethyl sulfoxide, DMT1: Divalent metal transporter 1, dSfxn: Drosophila sideroflexin, ETC: Electron transport chain, Fe<sup>2+</sup>: Iron ferrous, Fe<sup>3+</sup>: Iron ferric, Fe-S: Iron-sulfur, FECH: Ferrochelatase, FeSFA: Fluorescence assay, FIN56: ferroptosis inducing 56, FLVCR1b: Feline leukemia virus subgroup C receptor 1, Fp: Flavoprotein, fpn-1.1: Ferroportin 1.1, Fsf1: Fungal sideroflexin 1, FtMt: Ferritin Mitochondrial, FXN: Frataxin, GDH: Glutamate dehydrogenase, Gpx4: Glutathione peroxidase 4, GTP: Guanosine Triphosphate, HBM: Heme Binding Motif, HEK: Human embryonic kidney, HO-1: Heme oxygenase-1, ISCs: Iron-sulfur clusters, IMM: Inner mitochondrial membrane, IMPC: International Mouse Phenotyping Consortium, IMS: Intermembrane space, IRE: Iron Response Elements, IRP1/2: Iron Related Protein 1 and 2, ISCU: Iron-sulfur cluster assembly enzyme, ISP: Iron-sulfur protein, LC-MS/MS: Liquid chromatography-coupled to tandem mass spectrometry, LPS: Lipopolysaccharide, LYRM7: LYR motif-containing protein 7, Madh5: Mothers against decapentaplegic homolog, MDA: Malondialdehyde, MEF: Mouse Embryonic Fibroblasts, MEL: Mouse erythroleukemia, Mfrn1/2: Mitoferrin 1/2, MnSOD: Manganese superoxide dismutase, NAD(P)<sup>+</sup>: Nicotinamide adenine dinucleotide phosphate, NADH: Nicotinamide adenine dinucleotide hydrogen, NCO4A: nuclear receptor coactivator 4, NDUFB8: NADH dehydrogenase [ubiquinone] 1 beta subcomplex subunit 8, NDUFS1: NADH dehydrogenase (ubiquinone) Fe-S protein 1, NDUFS7: NADH dehydrogenase (ubiquinone) Fe-S protein 7, NDUFS8: NADH dehydrogenase (ubiquinone) Fe-S protein 8, NDUFV1: NADH dehydrogenase [ubiquinone] flavoprotein 1, NFS1: nitrogen fixation 1 homolog (*S. cerevisiae*), NMJ: Neuromuscular

1004 junctions, NUDFV2: NADH dehydrogenase [ubiquinone] flavoprotein 2, OCM: One-carbon metabolism, OCR:  
1005 Oxygen Consumption Rates, OXPHOS: Oxidative Phosphorylation, PD: Parkinson's disease, PGB: Porphobilin-  
1006 ogen, PL-PUFA: phospholipid-bound polyunsaturated fatty acids, PPIX: Protoporphyrin IX, PPOX: Protopor-  
1007 phyrinogen oxidase, PTGS2: Prostaglandin-Endoperoxide Synthase 2, RC: Respiratory complexes, RCD: Reg-  
1008 ulated Cell death, RISP: Rieske iron-sulfur protein, ROS: Reactive oxygen species, RSL3: Ras-selective lethality  
1009 protein 3, SCHAD: Short-Chain 3-Hydroxyacyl-Coenzyme A, SDHA: Succinate dehydrogenase complex, subu-  
1010 nit A, SDHB: Succinate dehydrogenase complex, subunit B, SDHC: Succinate dehydrogenase complex, subunit  
1011 C, Ser: Serine, SFXN: Sideroflexins, SHMT2: Serine Hydroxymethyltransferase 2, SILAC: Stable isotope labeling  
1012 by amino acids, SIRT4: Sirtuin 4, SLC25A38 Solute carrier Family 25 Member 38, SLC25A39: Solute Carrier  
1013 Family 25 Member 39, SLC56: Solute carrier family, STEAP3: Six-Transmembrane Epithelial Antigen of Prostate  
1014 3, STED: Stimulation Emission Depletion, TCA: Tricarboxylic acid, TCC: Tricarboxylate carrier, TEM-EDX:  
1015 Transmission electron microscopy linked with energy-dispersive X-ray spectroscopy, TF: Transferrin, TFR1:  
1016 Transferrin receptor protein 1, TIM22: Translocase of Inner Mitochondrial Membrane 22, TTC19: Tetratricopep-  
1017 tide Repeat Domain 19, UQCC1-3: ubiquinol-cytochrome c reductase complex assembly factor 1, UQCRC2: Cy-  
1018 tochrome b-c1 complex subunit 2, UQCRFS1: Cytochrome b-c1 complex subunit Rieske, UROD: Uroporphyno-  
1019 gen decarboxylase, UROgenIII: Uroporphyrinogen III, UROS: Uroporphyrinogen Synthase

1020 **Author Contributions:** methodology, A.G.; data curation, N.T., J.M.H.; writing—original draft  
1021 preparation, N.T, J.M.H, N.L.; writing—review and editing, N.L, S.B and B.M.; supervision, pro-  
1022 ject administration, funding acquisition, N.L. All authors have read and agreed to the published  
1023 version of the manuscript.”

1024 **Funding:** This research was funded by UVSQ, EPHE and private funding collected by the UVSQ  
1025 Foundation. NL received a grant from the UVSQ (AAPSI2019 for the MITOSIDERO project). This  
1026 work was partly funded by ‘NeurATRIS ANR-11-INBS-0011’, of the French Investissements  
1027 d’Avenir Program run by the Agence Nationale pour la Recherche.

1028 **Acknowledgments:** We acknowledge all the members of the LGBC lab for their support and their  
1029 contribution to the good atmosphere at work. We are particularly grateful to Juliette Bertheault de  
1030 Noiron who helped with Fiji macros, Sebastien Szuplewski for its interesting scientific speeches,  
1031 Christine Wintz for technical assistance and Marie-Pierre Golinelli for giving us DFO. And finally,  
1032 many thanks to the people who support our research by donating at the UVSQ Foundation.

1033 **Conflicts of Interest:** The authors declare no conflict of interest.

## 1034 Appendix A

### 1035 A.1. Prediction of Heme Binding Motifs in SFXN1

1036 The computational tool *SeqD-HBM* ([131.220.139.55/SeqDHBM/](https://doi.org/10.13122/139.55/SeqDHBM/)) was used for the de-  
1037 termination of heme binding motifs in human SFXN1 (Uniprot entry Q96NB2). The de-  
1038 fault mode released 13 possible heme-coordination sites and the WESA mode, which  
1039 passes the sequence through a sequence-based solvent accessibility meta-predictor, gave  
1040 4 putative HBMs. These putative HBMs were further located on SFXN1 predicted struc-  
1041 ture, highlighting 4 sites that may transiently interact with heme (**Figure S1**). If our pre-  
1042 dictions are correct, two sites would be located in the matrix and the others would be in  
1043 the intermembrane space.

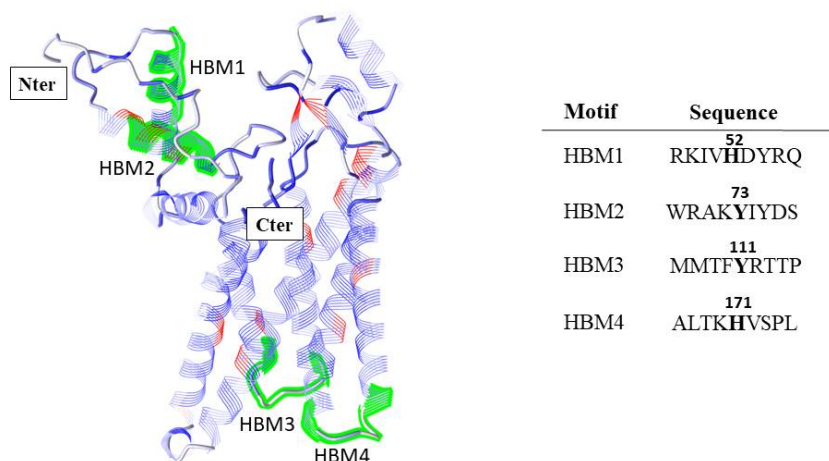


**Figure S1. Predicted HBMs in human SFXN1.** Left panel: The putative HBMs on SFXN1 predicted structure are highlighted (in green). Right panel: Sequences of the 9mer motifs in SFXN1 corresponding to predicted HBMs. The position of the potential heme-coordination site (Cys, His or Tyr) is shown (bold).

#### A.2. Mitochondrial labile iron staining with the MitoFerro-Green fluorescent probe

Prior to the staining, HT1080 cells were seeded in a 6-well plate and transiently transfected with a validated scrambled control siRNA (Control siRNA-A sc-37007, Santa Cruz Biotechnology, INC) or a pool of specific siRNA for SFXN1 (sc-91814, Santa Cruz Biotechnology, INC) using Interferin<sup>TM</sup> transfection reagent (Polyplus-transfection Inc., New York, NY) following manufacturer instructions. Briefly, a mix of siRNA and Interferin<sup>TM</sup> transfection reagent was prepared and incubated for 10 min at room temperature, and then, added to each well at a final concentration of 10 nM. Cells were incubated at 37°C under standard culture conditions and amplified. 24h post-transfection, cells were seeded in  $\mu$ -Slide 2 Well (Ibidi) and further incubated at 37°C under standard culture conditions for 24 h. The following day, cells were eventually treated with deferoxamine (DFO) with or without FeCl<sub>3</sub> for 1h30 or erastin for 6 h before adding the MitoFerro-Green probe (Dojindo, TEBU, France). MitoFerro-Green staining was done according to the manufacturer's recommendations. Live imaging images were acquired on a Leica TCS SPE confocal microscope with a 63X oil immersion objective (CYMAGES imaging facility, UVSQ). Image analysis of three independent experiments was done using ImageJ software with a macro developed in the lab.

## References

- Fleming, M.D. A Mutation in a Mitochondrial Transmembrane Protein Is Responsible for the Pleiotropic Hematological and Skeletal Phenotype of Flexed-Tail (*f/f*) Mice. *Genes & Development* **2001**, *15*, 652–657, doi:10.1101/gad.873001.
- Lenox, L.E.; Perry, J.M.; Paulson, R.F. BMP4 and Madh5 Regulate the Erythroid Response to Acute Anemia. *Blood* **2005**, *105*, 2741–2748, doi:10.1182/blood-2004-02-0703.
- Hegde, S.; Lenox, L.E.; Lariviere, A.; Porayette, P.; Perry, J.M.; Yon, M.; Paulson, R.F. An Intronic Sequence Mutated in Flexed-Tail Mice Regulates Splicing of Smad5. *Mamm Genome* **2007**, *18*, 852–860, doi:10.1007/s00335-007-9074-9.
- SLC56 Sideroflexins. IUPHAR/BPS Guide to PHARMACOLOGY 2020.
- Li, X.; Han, D.; Kin Ting Kam, R.; Guo, X.; Chen, M.; Yang, Y.; Zhao, H.; Chen, Y. Developmental Expression of Sideroflexin Family Genes in Xenopus Embryos. *Dev. Dyn.* **2010**, *239*, 2742–2747, doi:10.1002/dvdy.22401.
- Lockhart, P.J.; Holtom, B.; Lincoln, S.; Hussey, J.; Zimprich, A.; Gasser, T.; Wszolek, Z.K.; Hardy, J.; Farrer, M.J. The Human Sideroflexin 5 (SFXN5) Gene: Sequence, Expression Analysis and Exclusion as a Candidate for PARK3. *Gene* **2002**, *285*, 229–237.
- Miotto, G.; Tessaro, S.; Rotta, G.A.; Bonatto, D. In Silico Analyses of Fsf1 Sequences, a New Group of Fungal Proteins Orthologous to the Metazoan Sideroblastic Anemia-Related Sideroflexin Family. *Fungal Genet. Biol.* **2007**, *44*, 740–753, doi:10.1016/j.fgb.2006.12.004.

- 1081 8. Kory, N.; Wyant, G.A.; Prakash, G.; uit de Bos, J.; Bottanelli, F.; Pacold, M.E.; Chan, S.H.; Lewis, C.A.; Wang, T.; Keys, H.R.; et  
1082 al. SFXN1 Is a Mitochondrial Serine Transporter Required for One-Carbon Metabolism. *Science* **2018**, *362*, eaat9528, doi:10.1126/sci-  
1083 ence.aat9528.
- 1084 9. Mon, E.E.; Wei, F.-Y.; Ahmad, R.N.R.; Yamamoto, T.; Moroishi, T.; Tomizawa, K. Regulation of Mitochondrial Iron Homeosta-  
1085 sis by Sideroflexin 2. *The Journal of Physiological Sciences* **2019**, *69*, 359–373, doi:10.1007/s12576-018-0652-2.
- 1086 10. Gyimesi, G.; Hediger, M.A. Sequence Features of Mitochondrial Transporter Protein Families. *Biomolecules* **2020**, *10*, 1611,  
1087 doi:10.3390/biom10121611.
- 1088 11. Yang, J.; Anishchenko, I.; Park, H.; Peng, Z.; Ovchinnikov, S.; Baker, D. Improved Protein Structure Prediction Using Predicted  
1089 Interresidue Orientations. *Proc Natl Acad Sci USA* **2020**, *117*, 1496–1503, doi:10.1073/pnas.1914677117.
- 1090 12. Corpet, F. Multiple Sequence Alignment with Hierarchical Clustering. *Nucleic Acids Research* **1988**, *16*, 10881–10890,  
1091 doi:10.1093/nar/16.22.10881.
- 1092 13. Yoo, C.-M.; Rhee, H.-W. APEX, a Master Key to Resolve Membrane Topology in Live Cells. *Biochemistry* **2019**, acs.bio-  
1093 chem.9b00785, doi:10.1021/acs.biochem.9b00785.
- 1094 14. Lee, S.-Y.; Kang, M.-G.; Park, J.-S.; Lee, G.; Ting, A.Y.; Rhee, H.-W. APEX Fingerprinting Reveals the Subcellular Localization  
1095 of Proteins of Interest. *Cell Reports* **2016**, *15*, 1837–1847, doi:10.1016/j.celrep.2016.04.064.
- 1096 15. Acoba, M.G.; Selen Alpergin, E.S.; Renuse, S.; Fernández-del-Río, L.; Lu, Y.-W.; Clarke, C.F.; Pandey, A.; Wolfgang, M.J.; Clay-  
1097 pool, S.M. *The Mitochondrial Carrier SFXN1 Is Critical for Complex III Integrity and Cellular Metabolism*; Biochemistry, 2020;
- 1098 16. Jackson, T.D.; Hock, D.; Palmer, C.S.; Kang, Y.; Fujihara, K.M.; Clemons, N.J.; Thorburn, D.R.; Stroud, D.A.; Stojanovski, D. *The*  
1099 *TIM22 Complex Regulates Mitochondrial One-Carbon Metabolism by Mediating the Import of Sideroflexins*; Cell Biology, 2020;
- 1100 17. Azzi, A.; Glerum, M.; Koller, R.; Mertens, W.; Spycher, S. The Mitochondrial Tricarboxylate Carrier. *J Bioenerg Biomembr* **1993**,  
1101 *25*, 515–524, doi:10.1007/BF01108408.
- 1102 18. Miyake, S.; Yamashita, T.; Taniguchi, M.; Tamatani, M.; Sato, K.; Tohyama, M. Identification and Characterization of a Novel  
1103 Mitochondrial Tricarboxylate Carrier. *Biochemical and Biophysical Research Communications* **2002**, *295*, 463–468, doi:10.1016/S0006-  
1104 291X(02)00694-0.
- 1105 19. Kovaleva, G.Yu.; Bazykin, G.A.; Brudno, M.; Gelfand, M.S. COMPARATIVE GENOMICS OF TRANSCRIPTIONAL REGU-  
1106 LATION IN YEASTS AND ITS APPLICATION TO IDENTIFICATION OF A CANDIDATE ALPHA-ISOPROPYLMALATE TRANS-  
1107 PORTER. *Journal of Bioinformatics and Computational Biology* **2006**, *04*, 981–998, doi:10.1142/S0219720006002284.
- 1108 20. Wood, V.; Harris, M.A.; McDowall, M.D.; Rutherford, K.; Vaughan, B.W.; Staines, D.M.; Aslett, M.; Lock, A.; Bahler, J.; Kersey,  
1109 P.J.; et al. PomBase: A Comprehensive Online Resource for Fission Yeast. *Nucleic Acids Research* **2012**, *40*, D695–D699,  
1110 doi:10.1093/nar/gkr853.
- 1111 21. Lock, A.; Rutherford, K.; Harris, M.A.; Hayles, J.; Oliver, S.G.; Bähler, J.; Wood, V. PomBase 2018: User-Driven Reimplemen-  
1112 tation of the Fission Yeast Database Provides Rapid and Intuitive Access to Diverse, Interconnected Information. *Nucleic Acids Re-*  
1113 *search* **2019**, *47*, D821–D827, doi:10.1093/nar/gky961.
- 1114 22. Ye, X.; Xu, J.; Cheng, C.; Yin, G.; Zeng, L.; Ji, C.; Gu, S.; Xie, Y.; Mao, Y. Isolation and Characterization of a Novel Human  
1115 Putative Anemia-Related Gene Homologous to Mouse Sideroflexin. *Biochem. Genet.* **2003**, *41*, 119–125.
- 1116 23. Whittaker, M.M.; Penmatsa, A.; Whittaker, J.W. The Mtm1p Carrier and Pyridoxal 5'-Phosphate Cofactor Trafficking in Yeast  
1117 Mitochondria. *Archives of Biochemistry and Biophysics* **2015**, *568*, 64–70, doi:10.1016/j.abb.2015.01.021.
- 1118 24. Whittaker, J.W. Intracellular Trafficking of the Pyridoxal Cofactor. Implications for Health and Metabolic Disease. *Archives of*  
1119 *Biochemistry and Biophysics* **2016**, *592*, 20–26, doi:10.1016/j.abb.2015.11.031.
- 1120 25. Curcio, R.; Lunetti, P.; Zara, V.; Ferramosca, A.; Marra, F.; Fiermonte, G.; Cappello, A.R.; De Leonadis, F.; Capobianco, L.;  
1121 Dolce, V. Drosophila Melanogaster Mitochondrial Carriers: Similarities and Differences with the Human Carriers. *IJMS* **2020**, *21*,  
1122 6052, doi:10.3390/ijms21176052.
- 1123 26. Wang, J.; Youkharibache, P.; Zhang, D.; Lanczycki, C.J.; Geer, R.C.; Madej, T.; Phan, L.; Ward, M.; Lu, S.; Marchler, G.H.; et al.  
1124 ICn3D, a Web-Based 3D Viewer for Sharing 1D/2D/3D Representations of Biomolecular Structures. *Bioinformatics* **2020**, *36*, 131–135,  
1125 doi:10.1093/bioinformatics/btz502.
- 1126 27. Rivell, A.; Petralia, R.S.; Wang, Y.-X.; Mattson, M.P.; Yao, P.J. Sideroflexin 3 Is a Mitochondrial Protein Enriched in Neurons.  
1127 *Neuromol Med* **2019**, *21*, 314–321, doi:10.1007/s12017-019-08553-7.
- 1128 28. Hildick-Smith, G.J.; Cooney, J.D.; Garone, C.; Kremer, L.S.; Haack, T.B.; Thon, J.N.; Miyata, N.; Lieber, D.S.; Calvo, S.E.; Akman,  
1129 H.O.; et al. Macrocytic Anemia and Mitochondriopathy Resulting from a Defect in Sideroflexin 4. *Am. J. Hum. Genet.* **2013**, *93*, 906–  
1130 914, doi:10.1016/j.ajhg.2013.09.011.
- 1131 29. Fecher, C.; Trovò, L.; Müller, S.A.; Snaidero, N.; Wettmarshausen, J.; Heink, S.; Ortiz, O.; Wagner, I.; Kühn, R.; Hartmann, J.; et  
1132 al. Cell-Type-Specific Profiling of Brain Mitochondria Reveals Functional and Molecular Diversity. *Nat Neurosci* **2019**, *22*, 1731–1742,  
1133 doi:10.1038/s41593-019-0479-z.



- 1134 30. Sofou, K.; Hedberg-Oldfors, C.; Kollberg, G.; Thomsen, C.; Wiksell, Å.; Oldfors, A.; Tulinius, M. Prenatal onset of mitochon-  
1135 drial disease is associated with sideroflexin 4 deficiency. *Mitochondrion* **2019**, *47*, 76–81, doi:10.1016/j.mito.2019.04.012.
- 1136 31. Paul, B.T.; Tesfay, L.; Winkler, C.R.; Torti, F.M.; Torti, S.V. Sideroflexin 4 Affects Fe-S Cluster Biogenesis, Iron Metabolism,  
1137 Mitochondrial Respiration and Heme Biosynthetic Enzymes. *Sci Rep* **2019**, *9*, 19634, doi:10.1038/s41598-019-55907-z.
- 1138 32. Gylfe, A.E.; Katainen, R.; Kondelin, J.; Tanskanen, T.; Cajuso, T.; Hänninen, U.; Taipale, J.; Taipale, M.; Renkonen-Sinisalo, L.;  
1139 Järvinen, H.; et al. Eleven Candidate Susceptibility Genes for Common Familial Colorectal Cancer. *PLoS Genet* **2013**, *9*,  
1140 doi:10.1371/journal.pgen.1003876.
- 1141 33. Weston, C.; Klobusicky, J.; Weston, J.; Connor, J.; Toms, S.A.; Marko, N.F. Aberrations in the Iron Regulatory Gene Signature  
1142 Are Associated with Decreased Survival in Diffuse Infiltrating Gliomas. *PLoS ONE* **2016**, *11*, e0166593, doi:10.1371/jour-  
1143 nal.pone.0166593.
- 1144 34. Miller, L.D.; Coffman, L.G.; Chou, J.W.; Black, M.A.; Bergh, J.; D'Agostino, R.; Torti, S.V.; Torti, F.M. An Iron Regulatory Gene  
1145 Signature Predicts Outcome in Breast Cancer. *Cancer Res* **2011**, *71*, 6728–6737, doi:10.1158/0008-5472.CAN-11-1870.
- 1146 35. Wu, M.; Gu, J.; Zong, S.; Guo, R.; Liu, T.; Yang, M. Research Journey of Respirasome. *Protein Cell* **2020**, *11*, 318–338,  
1147 doi:10.1007/s13238-019-00681-x.
- 1148 36. Guo, R.; Gu, J.; Zong, S.; Wu, M.; Yang, M. Structure and Mechanism of Mitochondrial Electron Transport Chain. *Biomedical*  
1149 *Journal* **2018**, *41*, 9–20, doi:10.1016/j.bj.2017.12.001.
- 1150 37. Stiban, J.; So, M.; Kaguni, L.S. Iron-Sulfur Clusters in Mitochondrial Metabolism: Multifaceted Roles of a Simple Cofactor.  
1151 *Biochemistry Moscow* **2016**, *81*, 1066–1080, doi:10.1134/S0006297916100059.
- 1152 38. Barros, M.H.; McStay, G.P. Modular Biogenesis of Mitochondrial Respiratory Complexes. *Mitochondrion* **2020**, *50*, 94–114,  
1153 doi:10.1016/j.mito.2019.10.008.
- 1154 39. Letts, J.A.; Sazanov, L.A. Clarifying the Supercomplex: The Higher-Order Organization of the Mitochondrial Electron  
1155 Transport Chain. *Nat Struct Mol Biol* **2017**, *24*, 800–808, doi:10.1038/nsmb.3460.
- 1156 40. Ndi, M.; Marin-Buera, L.; Salvatori, R.; Singh, A.P.; Ott, M. Biogenesis of the Bc1 Complex of the Mitochondrial Respiratory  
1157 Chain. *Journal of Molecular Biology* **2018**, *430*, 3892–3905, doi:10.1016/j.jmb.2018.04.036.
- 1158 41. Sánchez, E.; Lobo, T.; Fox, J.L.; Zeviani, M.; Winge, D.R.; Fernández-Vizarra, E. LYRM7/MZM1L Is a UQCRRFS1 Chaperone  
1159 Involved in the Last Steps of Mitochondrial Complex III Assembly in Human Cells. *Biochimica et Biophysica Acta (BBA) - Bioenergetics*  
1160 **2013**, *1827*, 285–293, doi:10.1016/j.bbabi.2012.11.003.
- 1161 42. Tang, W.K.; Borgnia, M.J.; Hsu, A.L.; Esser, L.; Fox, T.; de Val, N.; Xia, D. Structures of AAA Protein Translocase Bcs1 Suggest  
1162 Translocation Mechanism of a Folded Protein. *Nat Struct Mol Biol* **2020**, *27*, 202–209, doi:10.1038/s41594-020-0373-0.
- 1163 43. Wang, Y.; Hekimi, S. Understanding Ubiquinone. *Trends in Cell Biology* **2016**, *26*, 367–378, doi:10.1016/j.tcb.2015.12.007.
- 1164 44. Visapää, I.; Fellman, V.; Vesa, J.; Dasvarma, A.; Hutton, J.L.; Kumar, V.; Payne, G.S.; Makarow, M.; Van Coster, R.; Taylor,  
1165 R.W.; et al. GRACILE Syndrome, a Lethal Metabolic Disorder with Iron Overload, Is Caused by a Point Mutation in BCS1L. *The*  
1166 *American Journal of Human Genetics* **2002**, *71*, 863–876, doi:10.1086/342773.
- 1167 45. Amorim, I.S.; Graham, L.C.; Carter, R.N.; Morton, N.M.; Hammachi, F.; Kunath, T.; Pennetta, G.; Carpanini, S.M.; Manson,  
1168 J.C.; Lamont, D.J.; et al. Sideroflexin 3 Is an  $\alpha$ -Synuclein-Dependent Mitochondrial Protein That Regulates Synaptic Morphology. *J.*  
1169 *Cell. Sci.* **2017**, *130*, 325–331, doi:10.1242/jcs.194241.
- 1170 46. Ducker, G.S.; Rabinowitz, J.D. One-Carbon Metabolism in Health and Disease. *Cell Metabolism* **2017**, *25*, 27–42,  
1171 doi:10.1016/j.cmet.2016.08.009.
- 1172 47. Minton, D.R.; Nam, M.; McLaughlin, D.J.; Shin, J.; Bayraktar, E.C.; Alvarez, S.W.; Sviderskiy, V.O.; Papagiannakopoulos, T.;  
1173 Sabatini, D.M.; Birsoy, K.; et al. Serine Catabolism by SHMT2 Is Required for Proper Mitochondrial Translation Initiation and Mainte-  
1174 nance of Formylmethionyl-TRNAs. *Molecular Cell* **2018**, *69*, 610–621.e5, doi:10.1016/j.molcel.2018.01.024.
- 1175 48. Antoniewicz, M.R. A Guide to <sup>13</sup>C Metabolic Flux Analysis for the Cancer Biologist. *Exp Mol Med* **2018**, *50*, 19,  
1176 doi:10.1038/s12276-018-0060-y.
- 1177 49. Plaitakis, A.; Kalef-Ezra, E.; Kotzamani, D.; Zaganas, I.; Spanaki, C. The Glutamate Dehydrogenase Pathway and Its Roles in  
1178 Cell and Tissue Biology in Health and Disease. *Biology* **2017**, *6*, 11, doi:10.3390/biology6010011.
- 1179 50. Smith, H.Q.; Li, C.; Stanley, C.A.; Smith, T.J. Glutamate Dehydrogenase, a Complex Enzyme at a Crucial Metabolic Branch  
1180 Point. *Neurochem Res* **2019**, *44*, 117–132, doi:10.1007/s11064-017-2428-0.
- 1181 51. Kurmi, K.; Haigis, M.C. Nitrogen Metabolism in Cancer and Immunity. *Trends in Cell Biology* **2020**, *30*, 408–424,  
1182 doi:10.1016/j.tcb.2020.02.005.
- 1183 52. Richardson, D.R.; Lane, D.J.R.; Becker, E.M.; Huang, M.L.-H.; Whitnall, M.; Rahmanto, Y.S.; Sheftel, A.D.; Ponka, P. Mitochon-  
1184 drial Iron Trafficking and the Integration of Iron Metabolism between the Mitochondrion and Cytosol. *Proceedings of the National*  
1185 *Academy of Sciences* **2010**, *107*, 10775–10782, doi:10.1073/pnas.0912925107.
- 1186 53. Torti, S.V.; Torti, F.M. Iron and Cancer: More Ore to Be Mined. *Nat Rev Cancer* **2013**, *13*, 342–355, doi:10.1038/nrc3495.

- 1187 54. Paul, B.T.; Manz, D.H.; Torti, F.M.; Torti, S.V. Mitochondria and Iron: Current Questions. *Expert Review of Hematology* **2017**, *10*,  
1188 65–79, doi:10.1080/17474086.2016.1268047.
- 1189 55. Kafina, M.D.; Paw, B.H. Intracellular Iron and Heme Trafficking and Metabolism in Developing Erythroblasts. *Metallomics*  
1190 **2017**, *9*, 1193–1203, doi:10.1039/C7MT00103G.
- 1191 56. Muckenthaler, M.U.; Galy, B.; Hentze, M.W. Systemic Iron Homeostasis and the Iron-Responsive Element/Iron-Regulatory  
1192 Protein (IRE/IRP) Regulatory Network. *Annu. Rev. Nutr.* **2008**, *28*, 197–213, doi:10.1146/annurev.nutr.28.061807.155521.
- 1193 57. Tong, W.-H.; Rouault, T.A. Metabolic Regulation of Citrate and Iron by Aconitases: Role of Iron–Sulfur Cluster Biogenesis.  
1194 *Biometals* **2007**, *20*, 549–564, doi:10.1007/s10534-006-9047-6.
- 1195 58. Zhou, Z.D.; Tan, E.-K. Iron Regulatory Protein (IRP)-Iron Responsive Element (IRE) Signaling Pathway in Human Neuro-  
1196 degenerative Diseases. *Mol Neurodegener* **2017**, *12*, 75, doi:10.1186/s13024-017-0218-4.
- 1197 59. Lill, R.; Mühlhoff, U. Maturation of Iron-Sulfur Proteins in Eukaryotes: Mechanisms, Connected Processes, and Diseases.  
1198 *Annu. Rev. Biochem.* **2008**, *77*, 669–700, doi:10.1146/annurev.biochem.76.052705.162653.
- 1199 60. Beinert, H.; Kennedy, M.C.; Stout, C.D. Aconitase as Iron–Sulfur Protein, Enzyme, and Iron-Regulatory Protein. *Chem. Rev.*  
1200 **1996**, *96*, 2335–2374, doi:10.1021/cr950040z.
- 1201 61. Netz, D.J.A.; Stith, C.M.; Stümpfig, M.; Köpf, G.; Vogel, D.; Genau, H.M.; Stodola, J.L.; Lill, R.; Burgers, P.M.J.; Pierik, A.J.  
1202 Eukaryotic DNA Polymerases Require an Iron-Sulfur Cluster for the Formation of Active Complexes. *Nat Chem Biol* **2012**, *8*, 125–132,  
1203 doi:10.1038/nchembio.721.
- 1204 62. Rudolf, J.; Makrantonis, V.; Ingledew, W.J.; Stark, M.J.R.; White, M.F. The DNA Repair Helicases XPD and FancJ Have Essential  
1205 Iron-Sulfur Domains. *Molecular Cell* **2006**, *23*, 801–808, doi:10.1016/j.molcel.2006.07.019.
- 1206 63. Rouault, T.A. Biogenesis of Iron-Sulfur Clusters in Mammalian Cells: New Insights and Relevance to Human Disease. *Disease*  
1207 *Models & Mechanisms* **2012**, *5*, 155–164, doi:10.1242/dmm.009019.
- 1208 64. Guengerich, F.P. Cytochrome P450 Research and *The Journal of Biological Chemistry*. *J. Biol. Chem.* **2019**, *294*, 1671–1680,  
1209 doi:10.1074/jbc.TM118.004144.
- 1210 65. Lin, Y.-W. Structure and Function of Heme Proteins Regulated by Diverse Post-Translational Modifications. *Archives of Bio-*  
1211 *chemistry and Biophysics* **2018**, *641*, 1–30, doi:10.1016/j.abb.2018.01.009.
- 1212 66. Poulos, T.L. Heme Enzyme Structure and Function. *Chem. Rev.* **2014**, *114*, 3919–3962, doi:10.1021/cr400415k.
- 1213 67. Ajioka, R.S.; Phillips, J.D.; Kushner, J.P. Biosynthesis of Heme in Mammals. *Biochimica et Biophysica Acta (BBA) - Molecular Cell*  
1214 *Research* **2006**, *1763*, 723–736, doi:10.1016/j.bbamcr.2006.05.005.
- 1215 68. Stojanovski, B.M.; Hunter, G.A.; Na, I.; Uversky, V.N.; Jiang, R.H.Y.; Ferreira, G.C. 5-Aminolevulinic Synthase Catalysis: The  
1216 Catcher in Heme Biosynthesis. *Molecular Genetics and Metabolism* **2019**, *128*, 178–189, doi:10.1016/j.yimgme.2019.06.003.
- 1217 69. Swenson, S.A.; Moore, C.M.; Marcero, J.R.; Medlock, A.E.; Reddi, A.R.; Khalimonchuk, O. From Synthesis to Utilization: The  
1218 Ins and Outs of Mitochondrial Heme. *Cells* **2020**, *9*, 579, doi:10.3390/cells9030579.
- 1219 70. Hirayama, T.; Kadota, S.; Niwa, M.; Nagasawa, H. A Mitochondria-Targeted Fluorescent Probe for Selective Detection of Mi-  
1220 tochondrial Labile Fe(II). *Metallomics* **2018**, *10*, 794–801, doi:10.1039/C8MT00049B.
- 1221 71. Nishizawa, H.; Matsumoto, M.; Shindo, T.; Saigusa, D.; Kato, H.; Suzuki, K.; Sato, M.; Ishii, Y.; Shimokawa, H.; Igarashi, K.  
1222 Ferroptosis Is Controlled by the Coordinated Transcriptional Regulation of Glutathione and Labile Iron Metabolism by the Tran-  
1223 scription Factor BACH1. *J. Biol. Chem.* **2020**, *295*, 69–82, doi:10.1074/jbc.RA119.009548.
- 1224 72. Kwon, M.-Y.; Park, E.; Lee, S.-J.; Chung, S.W. Heme Oxygenase-1 Accelerates Erastin-Induced Ferroptotic Cell Death. *Oncotar-*  
1225 *get* **2015**, *6*, 24393–24403, doi:10.18632/oncotarget.5162.
- 1226 73. Ichikawa, Y.; Bayeva, M.; Ghanefar, M.; Potini, V.; Sun, L.; Mutharasan, R.K.; Wu, R.; Khechaduri, A.; Jairaj Naik, T.; Ardehali,  
1227 H. Disruption of ATP-Binding Cassette B8 in Mice Leads to Cardiomyopathy through a Decrease in Mitochondrial Iron Export.  
1228 *Proceedings of the National Academy of Sciences* **2012**, *109*, 4152–4157, doi:10.1073/pnas.1119338109.
- 1229 74. Lunetti, P.; Damiano, F.; De Benedetto, G.; Siculella, L.; Pennetta, A.; Muto, L.; Paradies, E.; Marobbio, C.M.T.; Dolce, V.;  
1230 Capobianco, L. Characterization of Human and Yeast Mitochondrial Glycine Carriers with Implications for Heme Biosynthesis and  
1231 Anemia. *Journal of Biological Chemistry* **2016**, *291*, 19746–19759, doi:10.1074/jbc.M116.736876.
- 1232 75. Ulrich, D.L.; Lynch, J.; Wang, Y.; Fukuda, Y.; Nachagari, D.; Du, G.; Sun, D.; Fan, Y.; Tsurkan, L.; Potter, P.M.; et al. ATP-  
1233 Dependent Mitochondrial Porphyrin Importer ABCB6 Protects against Phenylhydrazine Toxicity. *J. Biol. Chem.* **2012**, *287*, 12679–  
1234 12690, doi:10.1074/jbc.M111.336180.
- 1235 76. Yamamoto, M.; Arimura, H.; Fukushige, T.; Minami, K.; Nishizawa, Y.; Tanimoto, A.; Kanekura, T.; Nakagawa, M.; Akiyama,  
1236 S. -i.; Furukawa, T. Abcb10 Role in Heme Biosynthesis In Vivo: Abcb10 Knockout in Mice Causes Anemia with Protoporphyrin IX  
1237 and Iron Accumulation. *Molecular and Cellular Biology* **2014**, *34*, 1077–1084, doi:10.1128/MCB.00865-13.
- 1238 77. Wißbrock, A.; Paul George, A.A.; Brewitz, H.H.; Kühl, T.; Imhof, D. The Molecular Basis of Transient Heme-Protein Interac-  
1239 tions: Analysis, Concept and Implementation. *Bioscience Reports* **2019**, *39*, BSR20181940, doi:10.1042/BSR20181940.

- 1240 78. Paul George, A.A.; Lacerda, M.; Syllwasschy, B.F.; Hopp, M.-T.; Wißbrock, A.; Imhof, D. HeMoQuest: A Webserver for Qual-  
1241 itative Prediction of Transient Heme Binding to Protein Motifs. *BMC Bioinformatics* **2020**, *21*, 124, doi:10.1186/s12859-020-3420-2.
- 1242 79. Kubota, Y.; Nomura, K.; Katoh, Y.; Yamashita, R.; Kaneko, K.; Furuyama, K. Novel Mechanisms for Heme-Dependent Degrada-  
1243 tion of ALAS1 Protein as a Component of Negative Feedback Regulation of Heme Biosynthesis. *J. Biol. Chem.* **2016**, *291*, 20516–  
1244 20529, doi:10.1074/jbc.M116.719161.
- 1245 80. Tretter, L.; Adam-Vizi, V. Alpha-Ketoglutarate Dehydrogenase: A Target and Generator of Oxidative Stress. *Phil. Trans. R. Soc.*  
1246 *B* **2005**, *360*, 2335–2345, doi:10.1098/rstb.2005.1764.
- 1247 81. Bulteau, A.-L. Frataxin Acts as an Iron Chaperone Protein to Modulate Mitochondrial Aconitase Activity. *Science* **2004**, *305*,  
1248 242–245, doi:10.1126/science.1098991.
- 1249 82. Mochel, F.; Knight, M.A.; Tong, W.-H.; Hernandez, D.; Ayyad, K.; Taivassalo, T.; Andersen, P.M.; Singleton, A.; Rouault, T.A.;  
1250 Fischbeck, K.H.; et al. Splice Mutation in the Iron-Sulfur Cluster Scaffold Protein ISCU Causes Myopathy with Exercise Intolerance.  
1251 *The American Journal of Human Genetics* **2008**, *82*, 652–660, doi:10.1016/j.ajhg.2007.12.012.
- 1252 83. Taketani, S.; Kakimoto, K.; Ueta, H.; Masaki, R.; Furukawa, T. Involvement of ABC7 in the Biosynthesis of Heme in Erythroid  
1253 Cells: Interaction of ABC7 with Ferrochelatase. *Blood* **2003**, *101*, 3274–3280, doi:10.1182/blood-2002-04-1212.
- 1254 84. Gervason, S.; Larkem, D.; Mansour, A.B.; Botzanowski, T.; Müller, C.S.; Pecqueur, L.; Le Pavec, G.; Delaunay-Moisan, A.; Brun,  
1255 O.; Agramunt, J.; et al. Physiologically Relevant Reconstitution of Iron-Sulfur Cluster Biosynthesis Uncovers Persulfide-Processing  
1256 Functions of Ferredoxin-2 and Frataxin. *Nat Commun* **2019**, *10*, 3566, doi:10.1038/s41467-019-11470-9.
- 1257 85. van den Ecker, D.; Hoffmann, M.; Müting, G.; Maglioni, S.; Herebian, D.; Mayatepek, E.; Ventura, N.; Distelmaier, F. Caeno-  
1258 rhabditis Elegans ATAD-3 Modulates Mitochondrial Iron and Heme Homeostasis. *Biochemical and Biophysical Research Communica-*  
1259 *tions* **2015**, *467*, 389–394, doi:10.1016/j.bbrc.2015.09.143.
- 1260 86. Harel, T.; Yoon, W.H.; Garone, C.; Gu, S.; Coban-Akdemir, Z.; Eldomery, M.K.; Posey, J.E.; Jhangiani, S.N.; Rosenfeld, J.A.;  
1261 Cho, M.T.; et al. Recurrent De Novo and Biallelic Variation of ATAD3A , Encoding a Mitochondrial Membrane Protein, Results in  
1262 Distinct Neurological Syndromes. *The American Journal of Human Genetics* **2016**, *99*, 831–845, doi:10.1016/j.ajhg.2016.08.007.
- 1263 87. Chen, X.; Yu, C.; Kang, R.; Tang, D. Iron Metabolism in Ferroptosis. *Front. Cell Dev. Biol.* **2020**, *8*, 590226,  
1264 doi:10.3389/fcell.2020.590226.
- 1265 88. Wang, H.; Liu, C.; Zhao, Y.; Gao, G. Mitochondria Regulation in Ferroptosis. *European Journal of Cell Biology* **2020**, *99*, 151058,  
1266 doi:10.1016/j.ejcb.2019.151058.
- 1267 89. Battaglia, A.M.; Chirillo, R.; Aversa, I.; Sacco, A.; Costanzo, F.; Biamonte, F. Ferroptosis and Cancer: Mitochondria Meet the  
1268 “Iron Maiden” Cell Death. *Cells* **2020**, *9*, 1505, doi:10.3390/cells9061505.
- 1269 90. Dixon, S.J.; Lemberg, K.M.; Lamprecht, M.R.; Skouta, R.; Zaitsev, E.M.; Gleason, C.E.; Patel, D.N.; Bauer, A.J.; Cantley, A.M.;  
1270 Yang, W.S.; et al. Ferroptosis: An Iron-Dependent Form of Nonapoptotic Cell Death. *Cell* **2012**, *149*, 1060–1072,  
1271 doi:10.1016/j.cell.2012.03.042.
- 1272 91. Li, N.; Wang, W.; Zhou, H.; Wu, Q.; Duan, M.; Liu, C.; Wu, H.; Deng, W.; Shen, D.; Tang, Q. Ferritinophagy-Mediated Ferroptosis  
1273 Is Involved in Sepsis-Induced Cardiac Injury. *Free Radical Biology and Medicine* **2020**, *160*, 303–318, doi:10.1016/j.freeradbiomed.2020.08.009.
- 1275 92. Doll, S.; Freitas, F.P.; Shah, R.; Aldrovandi, M.; da Silva, M.C.; Ingold, I.; Goya Grocin, A.; Xavier da Silva, T.N.; Panzilius, E.;  
1276 Scheel, C.H.; et al. FSP1 Is a Glutathione-Independent Ferroptosis Suppressor. *Nature* **2019**, *575*, 693–698, doi:10.1038/s41586-019-  
1277 1707-0.
- 1278 93. Mancias, J.D.; Wang, X.; Gygi, S.P.; Harper, J.W.; Kimmelman, A.C. Quantitative Proteomics Identifies NCOA4 as the Cargo  
1279 Receptor Mediating Ferritinophagy. *Nature* **2014**, *509*, 105–109, doi:10.1038/nature13148.
- 1280 94. Tang, M.; Huang, Z.; Luo, X.; Liu, M.; Wang, L.; Qi, Z.; Huang, S.; Zhong, J.; Chen, J.-X.; Li, L.; et al. Ferritinophagy Activation  
1281 and Sideroflexin1-Dependent Mitochondria Iron Overload Is Involved in Apelin-13-Induced Cardiomyocytes Hypertrophy. *Free*  
1282 *Radical Biology and Medicine* **2019**, *134*, 445–457, doi:10.1016/j.freeradbiomed.2019.01.052.
- 1283 95. Hentze, M.W.; Caughman, S.W.; Casey, J.L.; Kodier, D.M.; Rouault, T.A.; Harford, J.B.; Klausner, R.D. A Model for the Struc-  
1284 ture and Functions of Iron-Responsive Elements. *Gene* **1988**, *72*, 201–208, doi:10.1016/0378-1119(88)90145-X.
- 1285 96. Campillos, M.; Cases, I.; Hentze, M.W.; Sanchez, M. SIREs: Searching for Iron-Responsive Elements. *Nucleic Acids Research*  
1286 **2010**, *38*, W360–W367, doi:10.1093/nar/gkq371.
- 1287 97. Henderson, B.R.; Menotti, E.; Bonnard, C.; Kühn, L.C. Optimal Sequence and Structure of Iron-Responsive Elements. Selection  
1288 of RNA Stem-Loops with High Affinity for Iron Regulatory Factor. *J Biol Chem* **1994**, *269*, 17481–17489.
- 1289 98. Henderson, B.R.; Menotti, E.; Kühn, L.C. Iron Regulatory Proteins 1 and 2 Bind Distinct Sets of RNA Target Sequences. *J Biol*  
1290 *Chem* **1996**, *271*, 4900–4908, doi:10.1074/jbc.271.9.4900.

- 1291 99. Butt, J.; Kim, H.Y.; Basilion, J.P.; Cohen, S.; Iwai, K.; Philpott, C.C.; Altschul, S.; Klausner, R.D.; Rouault, T.A. Differences in the  
1292 RNA Binding Sites of Iron Regulatory Proteins and Potential Target Diversity. *Proceedings of the National Academy of Sciences* **1996**, *93*,  
1293 4345–4349, doi:10.1073/pnas.93.9.4345.
- 1294 100. Ward, R.J.; Zucca, F.A.; Duyn, J.H.; Crichton, R.R.; Zecca, L. The Role of Iron in Brain Ageing and Neurodegenerative Disor-  
1295 ders. *The Lancet Neurology* **2014**, *13*, 1045–1060, doi:10.1016/S1474-4422(14)70117-6.
- 1296 101. Lee, J.-H.; Lee, M.-S. Brain Iron Accumulation in Atypical Parkinsonian Syndromes: In Vivo MRI Evidences for Distinctive  
1297 Patterns. *Front. Neurol.* **2019**, *10*, 74, doi:10.3389/fneur.2019.00074.
- 1298 102. Ayton, S.; Wang, Y.; Diouf, I.; Schneider, J.A.; Brockman, J.; Morris, M.C.; Bush, A.I. Brain Iron Is Associated with Accelerated  
1299 Cognitive Decline in People with Alzheimer Pathology. *Mol Psychiatry* **2020**, *25*, 2932–2941, doi:10.1038/s41380-019-0375-7.
- 1300 103. Bousejra-ElGarah, F.; Bijani, C.; Coppel, Y.; Faller, P.; Hureau, C. Iron(II) Binding to Amyloid- $\beta$ , the Alzheimer's Peptide. *Inorg.*  
1301 *Chem.* **2011**, *50*, 9024–9030, doi:10.1021/ic201233b.
- 1302 104. Derry, P.J.; Kent, T.A. Correlating Quantitative Susceptibility Mapping with Cognitive Decline in Alzheimer's Disease. *Brain*  
1303 **2017**, *140*, 2069–2072, doi:10.1093/brain/awx167.
- 1304 105. Boopathi, S.; Kolandaivel, P. Fe<sup>2+</sup> Binding on Amyloid  $\beta$ -Peptide Promotes Aggregation: Fe<sup>2+</sup> Promotes A $\beta$  Aggregation.  
1305 *Proteins* **2016**, *84*, 1257–1274, doi:10.1002/prot.25075.
- 1306 106. Uranga, R.M.; Salvador, G.A. Unraveling the Burden of Iron in Neurodegeneration: Intersections with Amyloid Beta Peptide  
1307 Pathology. *Oxidative Medicine and Cellular Longevity* **2018**, *2018*, 1–12, doi:10.1155/2018/2850341.
- 1308 107. Ott, S.; Dziadulewicz, N.; Crowther, D.C. Iron Is a Specific Cofactor for Distinct Oxidation- and Aggregation-Dependent A  
1309 Toxicity Mechanisms in a Drosophila Model. *Disease Models & Mechanisms* **2015**, *8*, 657–667, doi:10.1242/dmm.019042.
- 1310 108. Minjarez, B.; Calderón-González, K.G.; Rustarazo, M.L.V.; Herrera-Aguirre, M.E.; Labra-Barrios, M.L.; Rincon-Limas, D.E.; Del  
1311 Pino, M.M.S.; Mena, R.; Luna-Arias, J.P. Identification of Proteins That Are Differentially Expressed in Brains with Alzheimer's Dis-  
1312 ease Using ITRAQ Labeling and Tandem Mass Spectrometry. *J Proteomics* **2016**, *139*, 103–121, doi:10.1016/j.jpro.2016.03.022.
- 1313 109. Simunovic, F.; Yi, M.; Wang, Y.; Macey, L.; Brown, L.T.; Krichevsky, A.M.; Andersen, S.L.; Stephens, R.M.; Benes, F.M.;  
1314 Sonntag, K.C. Gene Expression Profiling of Substantia Nigra Dopamine Neurons: Further Insights into Parkinson's Disease Pathol-  
1315 ogy. *Brain* **2009**, *132*, 1795–1809, doi:10.1093/brain/awn323.
- 1316 110. Cahill, C.M.; Lahiri, D.K.; Huang, X.; Rogers, J.T. Amyloid Precursor Protein and Alpha Synuclein Translation, Implications  
1317 for Iron and Inflammation in Neurodegenerative Diseases. *Biochimica et Biophysica Acta (BBA) - General Subjects* **2009**, *1790*, 615–628,  
1318 doi:10.1016/j.bbagen.2008.12.001.
- 1319 111. Fang, Y.-Y.; Zeng, P.; Qu, N.; Ning, L.-N.; Chu, J.; Zhang, T.; Zhou, X.-W.; Tian, Q. Evidence of Altered Depression and De-  
1320 mentia-Related Proteins in the Brains of Young Rats after Ovariectomy. *J. Neurochem.* **2018**, *146*, 703–721, doi:10.1111/jnc.14537.
- 1321 112. Paul, B.T.; Tesfay, L.; Winkler, C.R.; Torti, F.M.; Torti, S.V. Sideroflexin 4 Affects Fe-S Cluster Biogenesis, Iron Metabolism,  
1322 Mitochondrial Respiration and Heme Biosynthetic Enzymes. *Sci Rep* **2019**, *9*, 19634, doi:10.1038/s41598-019-55907-z.
- 1323 113. Balachandran, R.C.; Mukhopadhyay, S.; McBride, D.; Veevers, J.; Harrison, F.E.; Aschner, M.; Haynes, E.N.; Bowman, A.B.  
1324 Brain Manganese and the Balance between Essential Roles and Neurotoxicity. *J. Biol. Chem.* **2020**, *295*, 6312–6329,  
1325 doi:10.1074/jbc.REV119.009453.
- 1326 114. Weiland, A.; Wang, Y.; Wu, W.; Lan, X.; Han, X.; Li, Q.; Wang, J. Ferroptosis and Its Role in Diverse Brain Diseases. *Mol*  
1327 *Neurobiol* **2019**, *56*, 4880–4893, doi:10.1007/s12035-018-1403-3.
- 1328 115. Do Van, B.; Gouel, F.; Jonneaux, A.; Timmerman, K.; Gelé, P.; Pétrault, M.; Bastide, M.; Laloux, C.; Moreau, C.; Bordet, R.; et  
1329 al. Ferroptosis, a Newly Characterized Form of Cell Death in Parkinson's Disease That Is Regulated by PKC. *Neurobiology of Disease*  
1330 **2016**, *94*, 169–178, doi:10.1016/j.nbd.2016.05.011.
- 1331 116. Zhang, Y.-H.; Wang, D.-W.; Xu, S.-F.; Zhang, S.; Fan, Y.-G.; Yang, Y.-Y.; Guo, S.-Q.; Wang, S.; Guo, T.; Wang, Z.-Y.; et al.  $\alpha$ -  
1332 Lipoic Acid Improves Abnormal Behavior by Mitigation of Oxidative Stress, Inflammation, Ferroptosis, and Tauopathy in P301S Tau  
1333 Transgenic Mice. *Redox Biology* **2018**, *14*, 535–548, doi:10.1016/j.redox.2017.11.001.
- 1334 117. Hambright, W.S.; Fonseca, R.S.; Chen, L.; Na, R.; Ran, Q. Ablation of Ferroptosis Regulator Glutathione Peroxidase 4 in Fore-  
1335 brain Neurons Promotes Cognitive Impairment and Neurodegeneration. *Redox Biology* **2017**, *12*, 8–17, doi:10.1016/j.redox.2017.01.021.
- 1336 118. Country, M.W. Retinal Metabolism: A Comparative Look at Energetics in the Retina. *Brain Research* **2017**, *1672*, 50–57,  
1337 doi:10.1016/j.brainres.2017.07.025.
- 1338 119. Picard, E.; Daruich, A.; Youale, J.; Courtois, Y.; Behar-Cohen, F. From Rust to Quantum Biology: The Role of Iron in Retina  
1339 Physiopathology. *Cells* **2020**, *9*, 705, doi:10.3390/cells9030705.
- 1340 120. Bigot, K.; Gondouin, P.; Bénard, R.; Montagne, P.; Youale, J.; Piazza, M.; Picard, E.; Bordet, T.; Behar-Cohen, F. Transferrin  
1341 Non-Viral Gene Therapy for Treatment of Retinal Degeneration. *Pharmaceutics* **2020**, *12*, 836, doi:10.3390/pharmaceutics12090836.

- 1342 121. Chen, B.; Aredo, B.; Ding, Y.; Zhong, X.; Zhu, Y.; Zhao, C.X.; Kumar, A.; Xing, C.; Gautron, L.; Lyon, S.; et al. Forward Genetic  
1343 Analysis Using OCT Screening Identifies *Sfn3* Mutations Leading to Progressive Outer Retinal Degeneration in Mice. *Proc Natl Acad*  
1344 *Sci USA* **2020**, *117*, 12931–12942, doi:10.1073/pnas.1921224117.

1345